



8.1 Anatomic and Physiologic Considerations

The pulmonary system consists of the lungs, airways, pulmonary and bronchial circulation, and chest wall. The lungs consist of lobes, three in the right (upper, middle, and lower) and two in the left lung (upper and lower). Each lobe is again divided into segments and lobules (Fig. 8.1). The airway system consists of upper airways (nasopharynx and oropharynx) and lower airways (trachea, bronchi, bronchioles, and alveolar ducts) connected by the larynx (Fig. 8.2).

8.1.1 Respiratory Airways

The *upper airways* are lined by a ciliated mucosa, richly supplied with blood, which warm and humidify the inspired air and get rid of foreign particles. The air normally flows by way of the nose, nasopharynx, and oropharynx to the lower airways. When the nose is obstructed or additional flow of air is needed, as during exercise, air flows via the mouth and oropharynx to the lower airways. Foreign particle removal and humidification are not efficient with mouth breathing as

compared with the usual breathing through the nose.

The *lower airways* are formed of a conducting system and a gas exchange system (Fig. 8.3). The trachea divides into two main bronchi at the carina, and each bronchus enters the corresponding lung at the hilum along with the pulmonary blood vessels and lymphatic channels. The trachea measures up to 25 cm in length and 2.5 cm in diameter. The right main bronchus extends to the right lung more vertically than the left bronchus to the left lung. This explains the more frequent aspiration of foreign material in the right side. At the hila, the bronchi divide to lobar bronchi, then segmental and subsegmental bronchi, and then into smaller bronchioles, and at the 16th division, the tracheobronchial tree ends in the tiny terminal bronchioles which form the ends of the conducting airways and are followed by the gas exchange airways. The lung segments are individual units with their bronchovascular supply; hence, they can be individually resected. The airways responsible for conducting air from outside the body into the lungs are lined by ciliated mucous membranes. The cilia, which are hairlike projections, act as sweepers to prevent dust and foreign particles from passing distally into the lungs. Damage to the respiratory epithelium and its cilia allows bacteria and viruses to proliferate and induce infection.

The gas exchange airways start where the terminal bronchioles divide further into smaller,

A. H. Elgazzar (✉) · N. Alnafisi
Department of Nuclear Medicine, Faculty of
Medicine, Kuwait University, Kuwait City, Kuwait

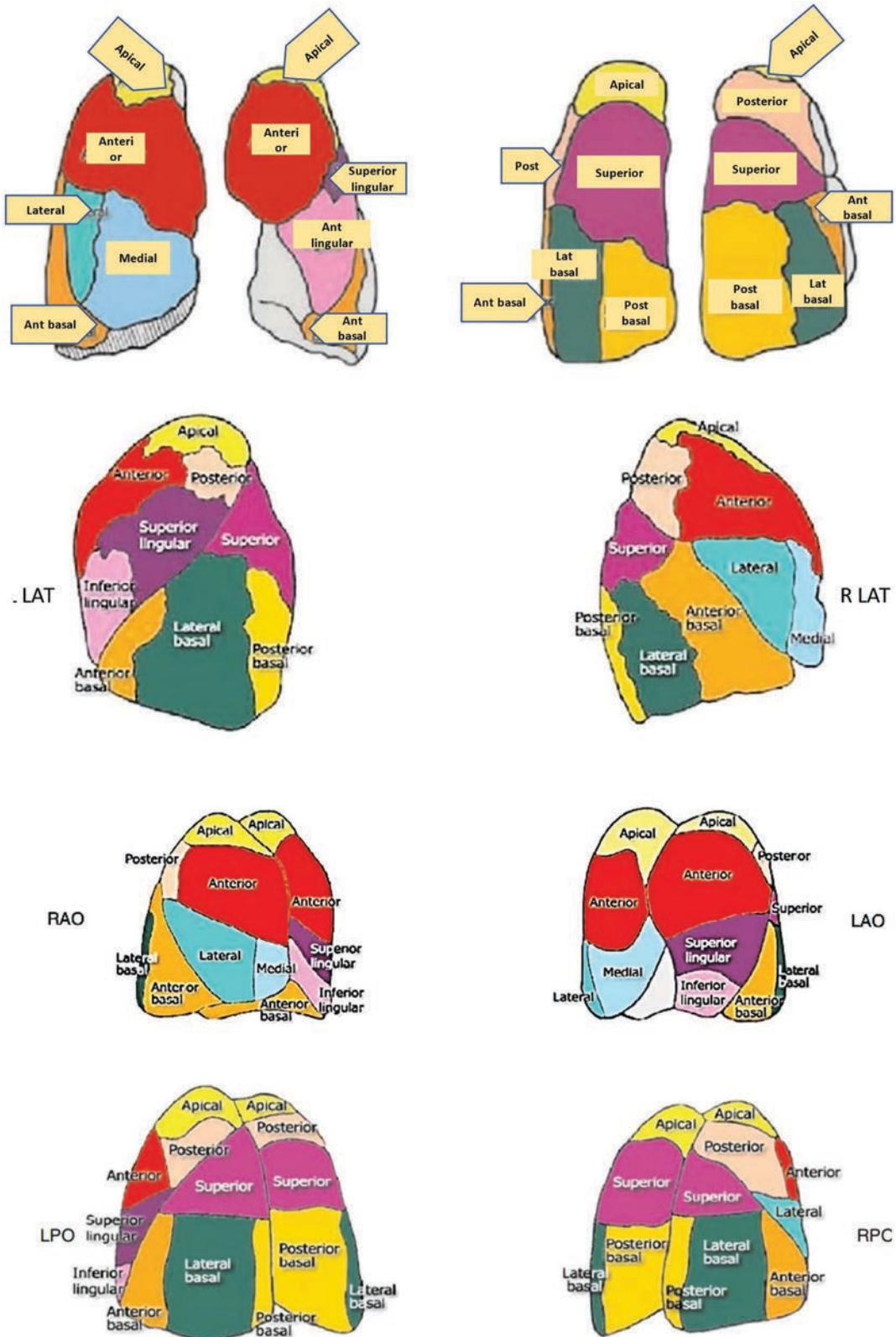


Fig. 8.1 Diagram of the lobes and segments of the lungs

Fig. 8.2 Simple diagram of the upper and lower airways

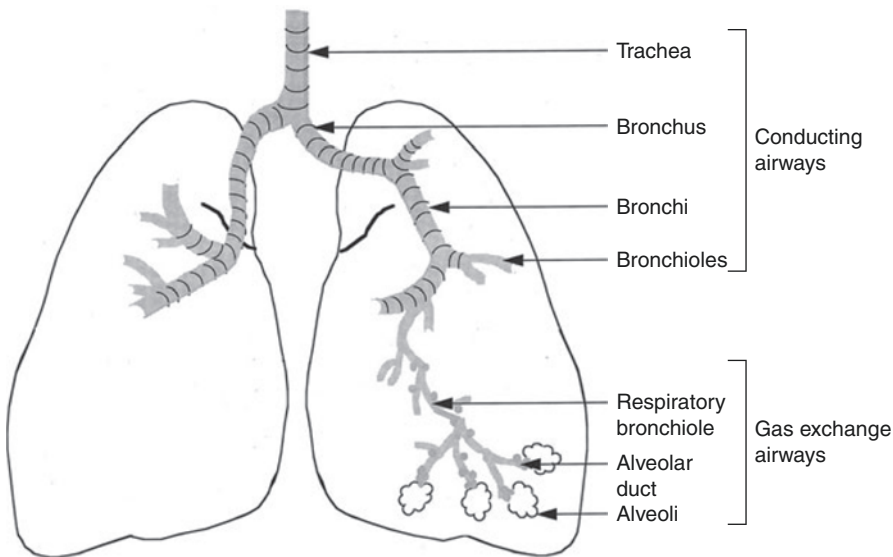
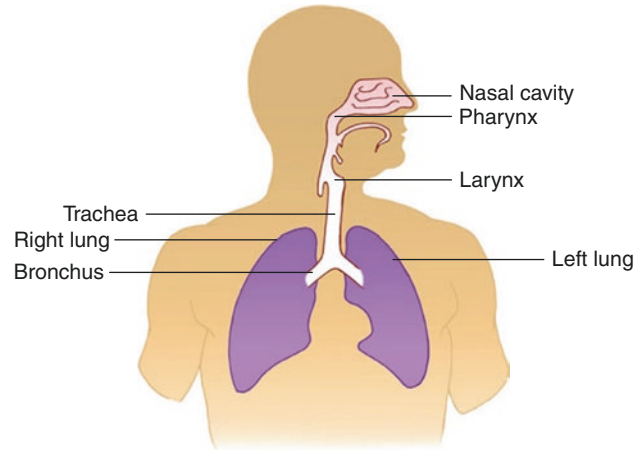


Fig. 8.3 The trachea, bronchi, and bronchioles form the tracheobronchial tree, so-called since it resembles an inverted tree. The conducting system is composed of the trachea, bronchi, and bronchioles up to the 16th division

and is lined by ciliated mucosa. The gas exchange system consists of the more distal bronchioles (respiratory) and the alveoli that are lined by nonciliated mucus membrane

respiratory bronchioles which include increasing numbers of alveoli as the division progresses. By the 23rd division, the respiratory bronchioles end in alveolar ducts that lead to alveolar sacs which are made up of numerous alveoli. The alveoli are extremely thin-walled sacs surrounded by capillaries and are the primary site of gas exchange. At birth there are approximately 25 million alveoli; this increases to 300 million in adults. The alveoli are lined by type I alveolar cells that provide structure to the alveolar wall and type II cells that

secrete a lipoprotein, the surfactant which coats the alveolar inner surface and aids its expansion during inspiration [1].

Ventilation describes the process by which air flows in and out of the gas exchange airways. Ventilation is involuntary most of the time and is controlled by the sympathetic and parasympathetic autonomic nervous systems, which adjust the caliber of the airway via contraction and relaxation of the bronchial smooth muscle and control the depth and rate of ventilation.

The nose and trachea trap most particles of more than 10 μm in diameter, while the cilia of the bronchi and bronchioles pick up particles 2–10 μm in diameter that are deposited in these airways. Smaller particles remain airborne till they are deposited in the alveoli and removed by macrophages. Extremely small particles behave as a gas and are breathed out. This is the basis of scintigraphic ventilation studies using radioactive aerosols and gases. The flow of oxygen through the $^{99\text{m}}\text{Tc}$ DTPA reservoir should create small aerosol particles to be airborne and deposited distally in the alveoli. Larger particles are deposited in the more proximal airways and influence the quality of ventilation studies. This also explains the longer biologic clearance of aerosols compared with radioactive gases, which are breathed out without deposition.

8.1.2 Pulmonary Vasculature

The lung is supplied by two different blood circulations. The pulmonary circulation is a low-pressure, low-resistance system through which oxygen enters and carbon dioxide is removed. The bronchial circulation is a part of the high-pressure systemic circulation that supplies oxygenated blood to the lung tissue itself.

The pulmonary circulation contains the vast majority of blood present in the lung, and since it has lower pressure than systemic circulation, its vessels have a thinner muscle layer. The mean pulmonary artery pressure is 18 mmHg, compared with 90 mmHg for the aorta. The gas exchange airways are served by this pulmonary circulation, which is considered a separate division of the circulatory system. The pulmonary circulation is carried through the pulmonary artery, which branches out to two main pulmonary arteries, one to each lung, entering at the hilum. It then divides progressively into smaller branches, following the branches of the bronchial tree to the smallest, precapillary arterioles, which divide to form a capillary network surrounding the alveoli. The membrane that surrounds the alveoli and contains the capillaries is called the alveolocapillary membrane [2].

The precapillary arterioles are approximately 35 μm in diameter and number approximately

300 million in adults. The capillaries, 7–10 μm in diameter, number 300 billion in adults. The more proximal terminal arterioles have a diameter of approximately 100 μm . This basic anatomical fact is important in determining the size of particles injected for perfusion studies; they should be less than 100 μm to prevent blocking of the terminal arterioles [3].

Although the pulmonary circulation is innervated by the autonomic nervous system, vasodilation and vasoconstriction are controlled mainly by local and humoral factors, particularly arterial oxygenation, and acid–base balance. Vasoconstriction of the pulmonary arterial system occurs secondary to alveolar hypoxia and acidemia and by the presence of inflammatory mediators such as histamine, bradykinin, serotonin, and prostaglandin.

The bronchial circulation, on the other hand, carries approximately 5% of the blood coming to the lungs and is part of the systemic circulation. In contrast to the pulmonary circulation, it does not participate in gas exchange. It supplies the tracheobronchial tree, large pulmonary vessels, and other structures of the lungs, including the pleurae, with blood.

8.1.3 Respiratory Function

The major function of the respiratory system is to oxygenate the blood and remove waste products of the body in the form of carbon dioxide. Oxygen in the inhaled air diffuses from the alveoli into the surrounding blood in the capillaries, where it attaches to hemoglobin molecules and red blood cells and is carried to the various tissues of the body. Carbon dioxide, on the other hand, as a waste product of cellular metabolism, diffuses in the opposite direction, from the blood in capillaries into the alveoli, and is removed from the body during expiration.

The respiration is controlled by the respiratory center in the medulla at the base of the brain. The respiratory center in the brain stem sends impulses to respiratory muscles to contract and relax. The respiratory center also receives impulses from two main types of peripheral receptors, neuro- and chemoreceptors.

Neuroreceptors (lung receptors) monitor the mechanical aspects of ventilation such as the need to expel unwanted substances and expansion of the lungs. The chemoreceptors in the brain circulatory system monitor the pH status of the cerebrospinal fluid and arterial oxygen content (PO_2) to regulate ventilation accordingly.

Any change in the carbon dioxide in the blood will affect the rate and depth of respiration. A slight increase in carbon dioxide concentration in the blood increases the rate and depth of respiration, such as when the individual exercises, since the accumulated waste gas must be removed from the body.

This increase in respiratory rate and depth is secondary to the stimulation of the muscles of respiration, which include the diaphragm and the intercostal muscles, by the respiratory center. Contraction of these muscles causes the volume of the chest cavity to increase, with a consequent drop in the pressure within the lungs, and forces air to move into the tracheobronchial tree. When these respiratory muscles relax, the volume of the chest cavity decreases, the pressure increases, and the air is pushed out of the lungs. When breathing is difficult, or in patients with obstructive airway disease, special muscles of expiration, abdominal and internal intercostal muscles, may be additionally needed.

8.1.4 Distribution of Ventilation and Perfusion

Normally, the lower zones of the lungs are better perfused and ventilated because of the effect of gravity. This gradient is more pronounced in perfusion than in ventilation (Fig. 8.4). This

physiological fact will usually cause the perfusion to appear less than the ventilation in the lung apices on scintigraphy. This should not be confused with a mismatching pattern. ^{99m}Tc -macroaggregated albumin (MAA) is injected for perfusion imaging while the patient is in the supine position to minimize the gradient. Injection while the patient is taking a deep breath also helps.

8.2 Pulmonary Embolic Disease

Venous thromboembolism, clinically presenting as DVT or PE, is the third most frequent acute cardiovascular syndrome globally with around ten million cases per year worldwide [5, 6]. The true incidence of PE is unknown, but in the USA, it is estimated that nearly one-third of hospitalized patients are at risk of developing venous thromboemboli and up to 600,000 cases of VTE are diagnosed per year [7].

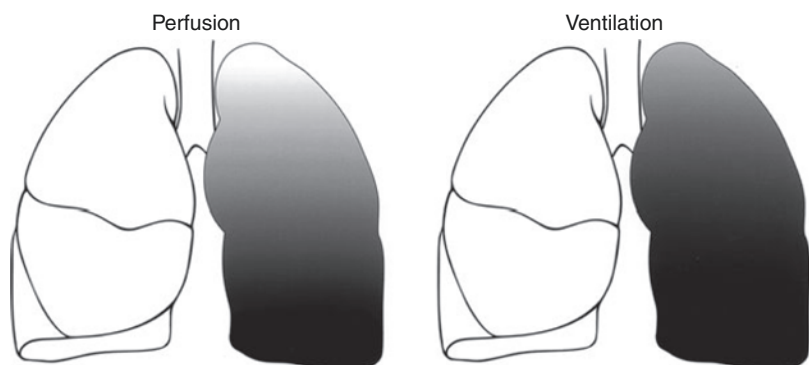
Pulmonary embolism is potentially fatal and the most common pathological condition involving the lungs of hospitalized patients. The majority of fatal emboli are not recognized or suspected prior to death.

8.2.1 Pathogenesis and Risk Factors

The vast majority of pulmonary emboli are thromboemboli originating from deep veins mostly from lower extremity [8, 9].

Fat, air, or tumor emboli are rare [10]. Fat emboli are reported with long bone fractures and liposuction, while air emboli occur in cardiac and

Fig. 8.4 The gradient pattern in perfusion and ventilation of the lungs. (From Elgazzar et al. [4] with permission)



neurosurgeries. Renal cell carcinoma with invasion reaching inferior vena cava is a clinical setting that may lead to tumor emboli. Data indicate that 90% of pulmonary thromboemboli originate from the lower extremities and pelvis. The remainder comes from thrombi that occur in the right side of the heart or in bronchial or cervical veins. Embolization and symptomatology are proportional to how proximal is the vein that contains the thrombus. The vast majority of pulmonary thromboemboli originating from thrombi of the lower extremities come more frequently from the thigh and pelvis (75%) than from smaller veins of the calf and feet [9, 11, 12]. Only 6% of the time upper extremity DVTs cause PE [13]. Septic embolus refers to an infected thromboembolus which occurs either on site or secondary to detachment of an infected vein thrombus of the lower extremities. The risk of pulmonary embolus is also directly related to the presence of a residual clot at the site of a venous thrombus [14].

Recently a common, yet not novel, risk factor for thromboembolism and PE is established with the Corona Virus Disease (COVID 2019) infection. Early in COVID-19 pandemic, multiple clinical, pathological, laboratory, and imaging reports demonstrated an association between COVID-19 infection and coagulopathies. These coagulopathies manifested as PE or venous, arterial, and/or microvascular thrombosis which are associated with severe viral injury of lung endothelium. In the available early and limited data, coagulopathy was reported in up to 50% of patients with severe COVID-19 manifestations. Deep vein thrombosis and PE was reported in up to 40% of patients. Current evidence is limited by small retrospective studies, and the true prevalence of thrombosis in COVID-19 is yet to be evaluated.

Pathogenesis of viral coagulopathy in the previously known various coronavirus infections has been extensively investigated. Some of the mechanisms proven include platelets consumption, thrombin generation, and increased fibrin degradation product (FDP) leading to disseminated intravascular coagulation (DIC)-like syndrome.

The specific mechanisms increasing the risk of thrombotic complications in patient with COVID-19 is currently under extensive investigation. Many factors are considered including the high levels of D-dimer and FDPs, the high levels of proinflammatory cytokines, and the endothelial dysfunction associated with the infection. It is hypothesized that an imbalance between coagulation and inflammation may result in COVID-19 hypercoagulable state. It is also suggested that COVID-19 coagulopathy is distinct from sepsis induced DIC and it reflect dysregulated hemostasis [15–20].

8.2.2 Deep Venous Thrombosis

The best solution to the problem of embolism is to prevent it. However, prevention requires identification of those at risk. Perhaps the most important step in defining who is at risk for this disorder has been the recognition that pulmonary emboli arise from the sites of deep venous thrombosis, almost exclusively in the lower extremity veins. Therefore, those at risk for deep venous thrombosis are those at risk for pulmonary embolism. The classical risk triad elucidated by Virchow in the nineteenth century includes venous stasis, intimal injury, and alteration in coagulation. These are the primary factors in the pathogenesis of venous thrombosis. Deficiencies of antithrombin III, protein C, protein S, and protein Z are clearly important, as is the presence of lupus anticoagulant. There are other rarer conditions such as homocystinuria and deficiencies of the fibrinolytic system. More factors are being identified, but at the present time, up to 90% of all patients with thromboembolism have no identifiable coagulopathy. Thus, in most patients, some clinical states associated with venous stasis, intimal injury, or both are the basis for an increased risk of deep venous thrombosis. These clinical states include injury to the pelvis or lower extremities, surgery involving the lower extremities, all surgical procedures requiring prolonged (at least 30 min) general anesthesia, burns, pregnancy and the postpartum state, previous venous thrombosis with residual obstruction, right ventricular failure

Table 8.1 Risk factors for deep vein thrombosis and pulmonary thromboembolism^a

<i>Inherited factors</i>
1. Antithrombin deficiency
2. Protein C deficiency
3. Protein S deficiency
4. Factor V Leiden
5. Prothrombin gene mutation
<i>Acquired factors</i>
1. Postoperative state especially following operations on the abdomen and pelvis
2. Trauma, including fractures, particularly of the lower extremities
3. Neoplasms
4. Prior history of thromboembolic disease
5. Venous stasis
6. Vascular spasm
7. Intimal injury
8. Hypercoagulability states
9. Immobilization
10. Infection of the area in the immediate of veins
11. Heart disease, especially:
Myocardial infarction
Atrial fibrillation
Cardiomyopathy
Congestive heart failure
12. Pregnancy
13. Polycythemia
14. Hemorrhage
15. Obesity
16. Old age
17. Extensive varicose veins
18. Certain drugs such as oral contraceptives, estrogens
19. Following cerebrovascular accidents
20. Smoking
21. Central venous instrumentation within the past 3 months
22. Homocystinemia
23. Homocystinuria
24. Hyperlipidemia
25. Hypertension
26. COVID-19 disease

^a [7, 15–21]

of any cause, occupations in which prolonged venous stasis is involved, and any cause of immobility. Other risk factors are age (particularly above 70 years), obesity, cancer, and the use of estrogen-containing medications, neoplasm, infection in the immediate area of veins, and hypercoagulability (Table 8.1).

An important point to note is that risk factors should be regarded as cumulative, not independent. These factors allow the establishment of a “risk profile” for a given patient, a profile that conditions the intensity of prophylactic initiatives. The anatomical location of the deep venous thrombosis affects as well the likelihood of extending into a pulmonary embolism as noted earlier.

Venous thrombi appear to begin either in the vicinity of a venous valve, where eddy current arises, or at the site of intimal injury. Platelet aggregation and release of mediators initiate the sequence. With stasis, there is local accumulation of coagulation factors; the coagulation cascade is activated, and the characteristic red fibrin thrombus develops. Pathologically there will be a platelet nidus from which a large fibrin thrombus extends.

Regarding the natural history, one of three events can happen after the formation of the thrombus. First, the red thrombus grows explosively and obstructs the vein completely. This can happen even within a few minutes. Second, partial venous obstruction may occur. Blood flow therefore continues over the thrombus surface. Under this circumstance, thrombus growth tends to occur by the progressive layering of platelets and fibrin on the clot surface, pathologically seen as the lines of Zahn. Third, probably the most common scenario, a small thrombus is swept away before it reaches an appreciable size. It lodges in the pulmonary vasculature without symptoms.

Unless fibrinolytic resolution is prompt, organization of the thrombus begins within hours of formation. The thrombus is slowly replaced by granulation tissue. This process anchors the thrombus to the venous wall.

The dynamic battle between fibrinolysis and thrombus formation is fought out over a period of 7–10 days, at the end of which time either complete resolution has occurred or an endothelialized residual is present. At any time during this period, a portion or all of the thrombus can detach as an embolus. This risk is highest early, before significant dissolution or organization occur [12].

8.2.3 Pulmonary Thromboembolism

8.2.3.1 Consequences

Pulmonary thromboemboli occur more commonly in the lower lobes because of the preferential blood flow to these regions. This also applies to the right lung because of the straighter course of the pulmonary artery. Immediately after acute embolism, there is a decrease of perfusion distal to the occluded vessel along with a transient decrease of ventilation to the affected segment. The blood flow is diverted to the other portions of the lung, and pulmonary artery pressure may increase, although cardiac output usually remains stable. The resultant tissue ischemia disturbs certain metabolic functions of the lung such as the production of surfactant. Reduction of the surfactant concentration reduces the alveolar surface tension and may cause the atelectasis that often accompanies embolism. If the embolus completely occludes an artery or an arteriole and the collateral bronchial circulation is insufficient to sustain tissue viability, infarction occurs over 24–48 h. Pulmonary infarction with coagulative necrosis results in an area of radiographic opacity that requires an average of 20 days to resolve but occurs in less than 10–15% of patients with pulmonary embolism. There is significant inflammatory component in pulmonary infarcts which is the basis behind the reported significant FDG uptake in recent lung infarcts and can cause false-positive interpretation for lung malignancy [22]. More frequently, incomplete infarction with hemorrhage but without necrosis occurs. This type of injury resolves quickly and produces only transient radiographic opacities. Infarction always involves the pleural surface of the lung (peripheral) and more frequently involves the lower lobes than other sites.

The regional decrease in ventilation is due to local bronchoconstriction with a tendency for redistribution of ventilation away from the hypoperfused segment. This probably occurs due to decreased regional alveolar and airway carbon dioxide tension, which is the usual stimulus for bronchodilation. This hypocapnia is corrected quickly, since patients inhale carbon dioxide-rich

tracheal “dead space air” into the alveolar zones after the embolic event, raising the alveolar $p\text{CO}_2$ [12]. The release of neurohumoral factors, most importantly serotonin and thromboxane A_2 , also causes bronchoconstriction. These factors are released after embolization by activated platelets and mediate bronchospasm of small airways through their effects on the smooth muscles [23]. The ventilation of the hypoperfused areas returns to normal within several hours after acute embolism [24, 25]. This concept is the pathophysiological basis for the scintigraphic interpretation of ventilation and perfusion scans, which show segmental perfusion defects with preserved ventilation as a typical scintigraphic pattern for pulmonary embolism. Those showing only regions of matched perfusion and ventilation defects carry a low probability of pulmonary embolism if no chest X-ray abnormalities are noted at the same sites, since this pattern is more likely associated with nonembolic conditions and is more typical of parenchymal lung disease. Because patients with pulmonary emboli usually arrive at the hospital after normalization of the ventilation at the site of pulmonary emboli, the mismatching pattern is typical of pulmonary emboli. However, inpatients may have their V/Q scans within a short time after presentation and matching abnormalities may be associated with pulmonary emboli. This has to be borne in mind, and the duration of symptoms should be a factor in decision-making regarding the management of pulmonary embolism.

Some degree of arterial hypoxemia may also occur, one reason being the widening of the arteriovenous oxygen difference caused by acute right ventricular failure. Another reason is the enhanced perfusion of poorly ventilated or non-ventilated lung zones. Loss of pulmonary surfactant may add to the hypoxemia. Hyperventilation almost always occurs and may partly explain the normal levels of oxygen arterial pressure seen in 10–25% of patients with pulmonary emboli.

An increase in the resistance of the pulmonary arterial circulation, due primarily to mechanical blockage by numerous small emboli in the pulmonary vasculature and also to humorally mediated vasoconstriction, may follow pulmonary

emboli. These hemodynamic consequences may include increased pulmonary arterial resistance with elevated pulmonary arterial and right ventricular systolic pressures and hypoxemia. When pulmonary hypertension occurs, it indicates at least 25% obstruction of pulmonary vascular tree as assessed by angiography [26]. The higher the degree of obstruction, the more severe the abnormalities of the cardiopulmonary hemodynamics become. When over 50% of the pulmonary vasculature is included (massive pulmonary embolism), acute pulmonary hypertension and/or right ventricular failure (cor pulmonale) occurs [26]. Systemic hypoxemia results from pulmonary arteriovenous shunting and from perfusion of hypoventilated lung segments (V-P imbalances). The AV shunting accounts for the clinical observation that administration of 100% oxygen will only partially correct hypoxemia induced by pulmonary emboli [27].

The physiological consequences of pulmonary embolism depend on the size of the embolic mass and the general status of the pulmonary circulation. In young individuals with good cardiovascular function and good collateral circulation, thrombi of a large central vessel may be associated with only minimal functional impairment if

any. On the other hand, in patients with cardiovascular or severely debilitating diseases, pulmonary embolism may lead to infarction.

8.2.3.2 Resolution

Pulmonary emboli may, spontaneously or with treatment, fragment into smaller portions that travel distally and block smaller arterioles (Fig. 8.5). This may create new, smaller perfusion defects that are more peripherally located in comparison to the original defect caused by the original embolus. This pattern should not be mistaken for recurrent pulmonary emboli on a follow-up scan. If this pattern is the only interval change with no other defects seen in areas other than those in the vicinity of the distribution of the original embolus, it does not suggest recurrent emboli [26].

Resolution of pulmonary thromboembolus may start within hours. It can be seen on perfusion scans as early as 24 h and is progressively noted up to 3 months, with insignificant change after 6 months (Fig. 8.6). This is the basis of the recommendation that follow-up ventilation and perfusion scans are performed 3 months after the initial incident for evaluation of resolution and function as a baseline for future incidents to dif-

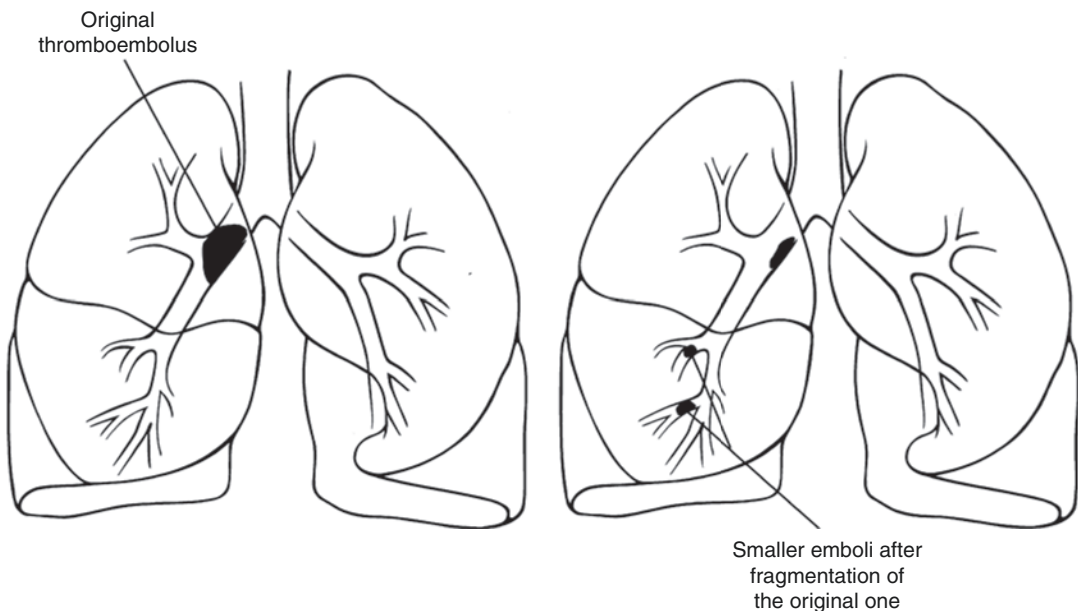


Fig. 8.5 The phenomenon of fragmentation of the thromboemboli. (From Elgazzar [4] with permission)

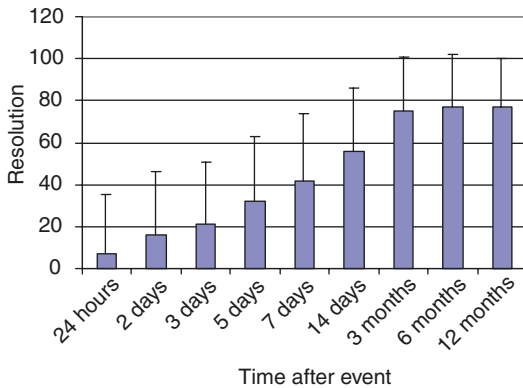


Fig. 8.6 Histogram illustrating the percent resolution of pulmonary emboli. Note that there is progressive increase of the percentage over time until 3 months after the event with no significant increase afterwards. (Data are based on the Urokinase Study [27, 28])

ferentiate between acute and unresolved old emboli. This resolution is dependent on the age of the patient, with complete resolution in young age groups and less complete and less significant resolution in older age groups [26, 27]. Other factors include age of the thromboembolus or length of time between formation of the embolus and the institution of proper anticoagulation. This is the basis behind the relatively recent trend of starting anticoagulant therapy in most patients with pulmonary emboli who have no contraindication for anticoagulation immediately when a pulmonary thromboembolus is suspected before finishing the workup for the condition. Anticoagulant therapy may then be stopped if the condition is excluded.

8.2.3.3 Chronic Pulmonary Thromboembolism

Incomplete resolution of acute pulmonary embolism is frequently observed and may rarely result in chronic thromboembolic pulmonary hypertension [29]. Chronic thromboembolic disease is characterized by intraluminal thrombus organization and fibrous stenosis or complete obliteration of pulmonary arteries. The consequence is an increased pulmonary vascular resistance resulting in pulmonary hypertension and progressive right heart failure. Pulmonary endarterectomy is the preferred treatment [30].

8.2.3.4 Recurrence

Pulmonary thromboemboli recur in up to 50% of patients [31], although the incidence in treated PIOPED patients was only 8.3% [32]. The vast majority of deaths among pulmonary embolism patients are due to recurrent emboli. In the PIOPED study population, it was found that nine of ten people who died had a recurrent pulmonary embolus [33]. Recurrence has been reported to occur at the same site as the original thromboembolus [34].

8.2.3.5 Diagnosis

The clinical diagnosis of pulmonary thromboembolism is difficult and unreliable, due to the non-specificity of its symptoms and signs as well as the laboratory and chest X-ray findings [35, 36]. Chest X-ray however must be obtained since it may show many parenchymal diseases and must be available for lung scan interpretation (Fig. 8.7). Pulmonary embolism may also be asymptomatic. In the literature, only 24% of fatal emboli were diagnosed antemortem (Table 8.2) [37–46]. Furthermore the presentation is commonly more difficult and atypical in older age group compared to younger patients [47, 48]. Accordingly only 24% of fatal emboli were diagnosed antemortem (Table 8.2). Data indicate that the mortality of pulmonary embolism is more than 30% if untreated. Promptly diagnosed and treated, emboli have a mortality of 2.5–8% [27, 28, 33]. The mortality of PE was found to vary among patients with or without cardiac disease. Paraskos et al. [49] reported survival rates at a mean follow-up period of 29 months of 19% among patients with prior congestive heart failure and 86% for those with no prior congestive heart failure. Pulmonary angiography is the most accurate modality for the diagnosis of pulmonary emboli with an accuracy of 96% [50]. However, angiography is invasive and is not suitable as a screening imaging modality for the disease.

D-dimer is a fibrin degradation product present in the blood after a thrombus is degraded through fibrinolysis. The blood test to determine D-dimer concentration helps diagnose thrombosis. Although a negative result practically rules out thrombosis, a positive result can indicate

Fig. 8.7 Normal chest X-ray illustrating the important structures that may show variants on perfusion scans

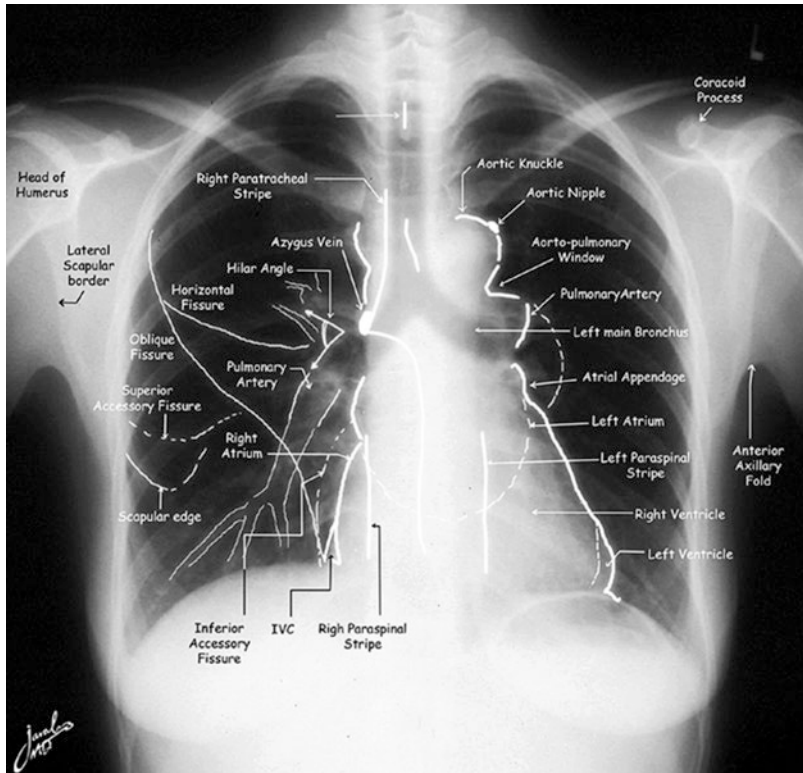


Table 8.2 Antemortem diagnosis of PE

Author	Year	No. (%) of cases with antemortem PE diagnosis
Stein and Henry [37]	1995	6/20 (30)
Morgenthaler and Ryu [38]	1995	29/92 (32)
Morpurgo and Schmid [39]	1991	26/92 (28)
Sperry et al. [40]	1990	275/812 (34)
Karwinski and Svendsen [41]	1989	267/1450 (18.4)
Gross et al. [42]	1988	7/18 (39)
Dismuke and Wagner [43]	1986	41/203 (20)
Goldhaber et al. [44]	1982	16/54 (30)
Rubio-Jurado et al. [45]	2003	9/66 (14)
Total		675/2807 (24)

thrombosis but does not rule out other potential causes. Its main use, therefore, is to exclude thromboembolic disease where the clinical probability is low. On the other hand, the positive predictive value of elevated D-dimer levels is low and D-dimer testing is not useful for confirmation of PE. D-dimer is also more frequently elevated in patients with cancer [51], in hospitalized patients [51–53], in severe infection or inflammatory disease, and during pregnancy [54].

Imaging

Scintigraphy remains the most cost-effective noninvasive screening modality. The major advantages include its ability to provide regional and quantitative information useful for the diagnosis, as well as for mapping to guide selective angiography if needed for the diagnosis. SPECT V/P scan has been strongly recommended as it is more accurate than planar imaging in establishing the diagnosis of PE even in the presence of

diseases such as COPD, heart failure, and pneumonia. Furthermore, adding low dose CT(SPECT/CT) improves the scan specificity especially in patients with other lung diseases [55].

CTPA is useful in detecting central emboli which has become the most commonly used modality in many centers at the expense of scintigraphy although data are still controversial for peripheral emboli [56–59]. Multislice CT was found to have no added value in patients with high-probability V/Q scans and has a comparable diagnostic value with SPECT V/Q scans [60]. CT also as a single study is not cost-effective [61]. It also requires the use of iodinated contrast media with its risk of renal failure and ionizing radiation with its risk of cancer induction [62, 63]. And it was also found to result in overdiagnosis of pulmonary emboli [58]. MRI pulmonary angiography will play a greater role [64]; however, the use of contrast media is still a shortcoming. In an experimental study, reversible PE was induced by inflating a nondetachable silicon balloon in the left pulmonary artery of five New Zealand white rabbits. MR V/Q scans were obtained prior to, during, and after balloon deflation. High-resolution contrast-enhanced MR pulmonary angiography was also used to confirm the occlusion of the pulmonary artery. Similar to radionuclide ventilation/perfusion technique, acute PE produced a mismatched defect in the MR V/Q scan. MRA verified the occlusive filling defect in the left pulmonary artery. The study suggests that high-resolution MRA and MR V/Q imaging of the lung is feasible and allows comprehensive assessment of pulmonary embolism in one imaging session [64]. Recently, non-contrast MRI has been studied in the diagnosis of PE [65]. There are growing evidence-based outcome data that Contrast-enhanced pulmonary MRA is a safe and accurate and radiation-free examination for the exclusion of clinically significant PE [66].

Scintigraphy is also valuable in pregnancy. When indicated low activity of 1 mCi (37 MBq) is used for perfusion, if the perfusion study is abnormal, then ventilation and chest X-ray (if not obtained earlier) are obtained as needed. Based upon the available data, there are no apparent short- or long-term consequences to the fetus

from the radiation received as a result of diagnostic ventilation/perfusion scintigraphy. For a V/Q scan, fetal dose would mostly come from tracer accumulating in the bladder, with some internal scatter from the lungs. Either Xenon133 or ^{99m}Tc agents can be used safely for the ventilation portion of the exam. Xenon103 has the advantage of not being excreted via the urine.

Scintigraphic Agents

Several agents have been used for ventilation (Table 8.3). Every agent has certain advantages and limitations. Xenon 133 (Fig. 8.8) is useful in evaluating obstructive airway disease. Krypton-81 (Fig. 8.9), ^{99m}Tc-DTPA (Fig. 8.10), and Technegas (Fig. 8.11) provide the ability to perform ventilation studies after the perfusion, particularly krypton-81. ^{99m}Tc-macroaggregated albumin is used for perfusion. For proper interpretation of lung perfusion/ventilation study, chest X-ray must be available and should be obtained within 12 h of the time of the scans.

Table 8.3 Ventilation agents

Agent	Advantages and limitations
<i>Aerosols</i>	
^{99m} Tc-DTPA aerosol	Lung half-clearance time = 58 min
	Pre- or post-perfusion
	Multiple projections
^{99m} Tc-pyrophosphate aerosol	Post perfusion
	Suitable for SPECT
Technegas	Multiple projections
	Good peripheral deposition
<i>Gases</i>	
Xenon-133	Ability to obtain single breath, equilibrium, and washout images
	Very sensitive for obstructive airway disease
	Only posterior view is possible in most patients
	Low energy of 81 keV
	Pre-perfusion acquisition
Krypton-81m	Expensive—available only in some areas
	Energy: 190 keV
	Half-life: 13 s
	Multiple views
	Pre- or post-perfusion

The particle size of ^{99m}Tc -macroaggregated albumin (^{99m}Tc -MAA) is generally between 10 and 90 μm (90% of particles), and no particles should be larger than 150 μm . ^{99m}Tc -MAA is injected slowly IV and lodges in precapillary arterioles, obstructing approximately 0.1% of their total number. The particles clear by enzymatic hydrolysis and are phagocytized by RE cells (the agent has a biologic half-life in the lungs of between 6 and 8 h). Normally, only 3–6% of the injected ^{99m}Tc -MAA will bypass the pulmonary vasculature. The critical organ is the

lungs which receive a dose of about 1 rad (1 cGy) from a typical 5 mCi dose. The kidneys and bladder receive moderate exposure largely from the excretion of degraded albumin.

^{99m}Tc -DTPA aerosol is commonly used for ventilation studies worldwide. Using an aerosol delivery system that generates submicronic particles, 30 mCi of Tc-DTPA in 3 mL of saline (3–5 min of rebreathing on the system with the oxygen at 8–10 L/min) delivers about 500–750 mCi of tracer to the lungs. This dose yields 100 K count images in about 2 min on a standard gamma

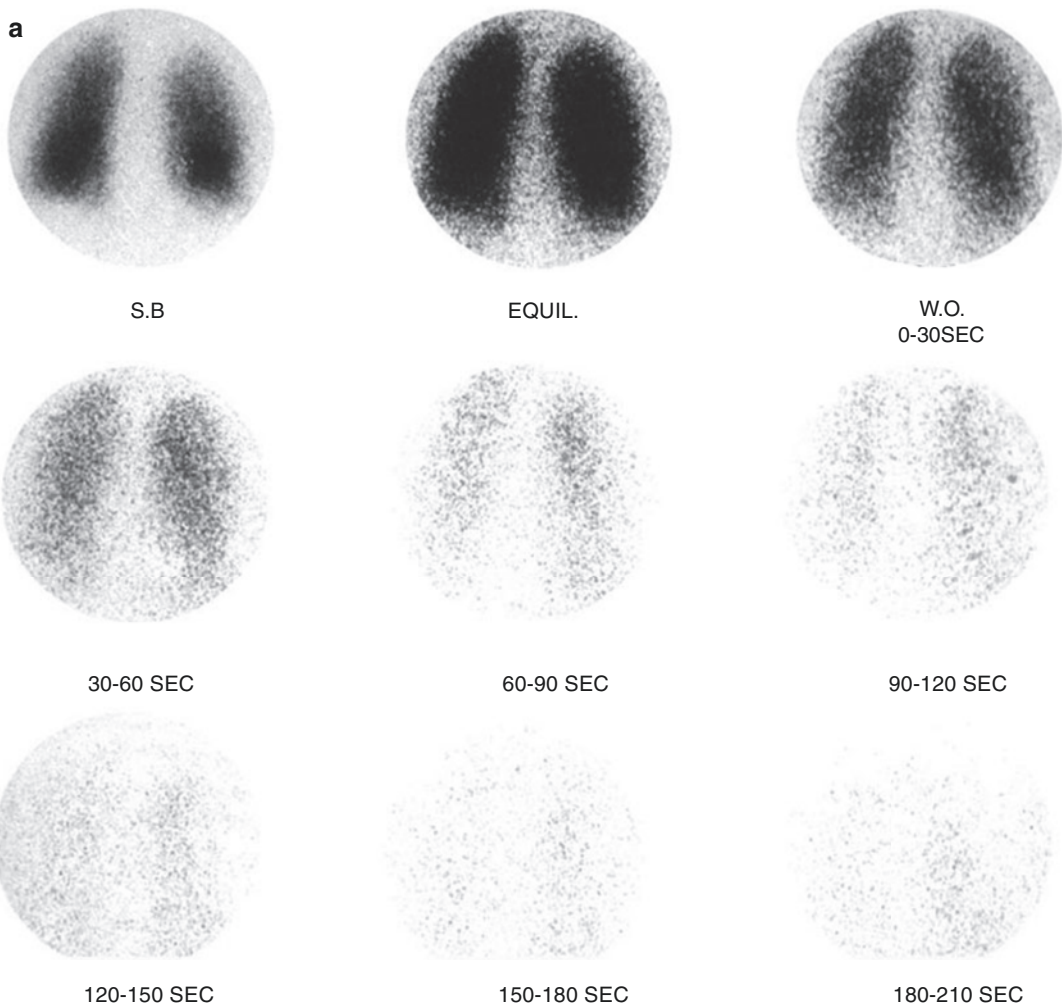


Fig. 8.8 (a, b) Xenon-133 ventilation studies. (a) Normal study with uniform distribution of the radiotracer in both lungs on single breath and equilibrium images. The washout images reveal prompt clearance with no significant

retained activity. (b) Washout images of a patient with obstructive airway disease showing retained activity in lower zones of both lungs by the end of the study

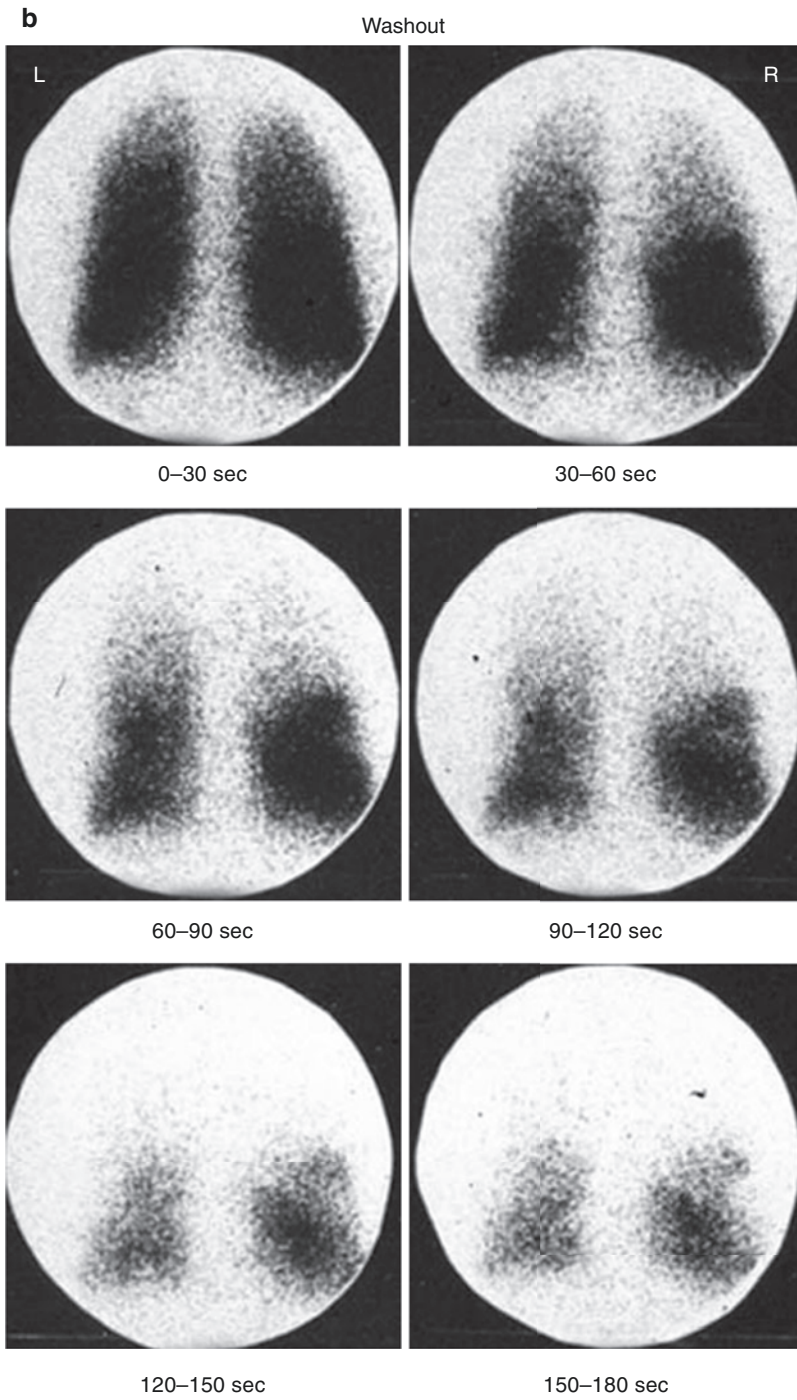


Fig. 8.8 (continued)

Fig. 8.9 Representative images of krypton-81 ventilation study obtained post perfusion. Note the good quality of images. The shown anterior and left posterior oblique (LPO) images illustrate the ability to evaluate the ventilation status at the regions of the perfusion abnormalities seen on the same projections

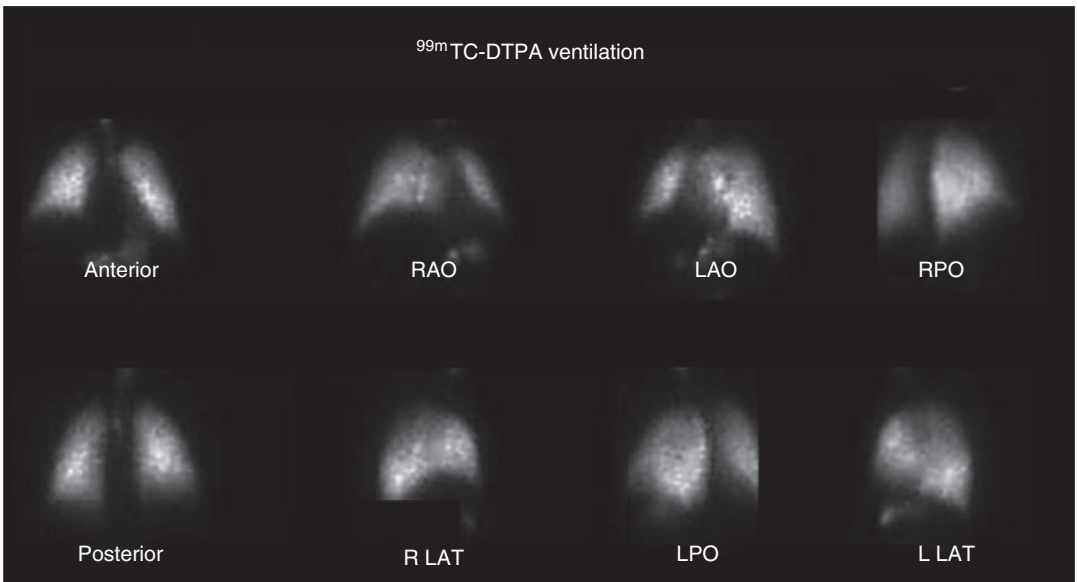
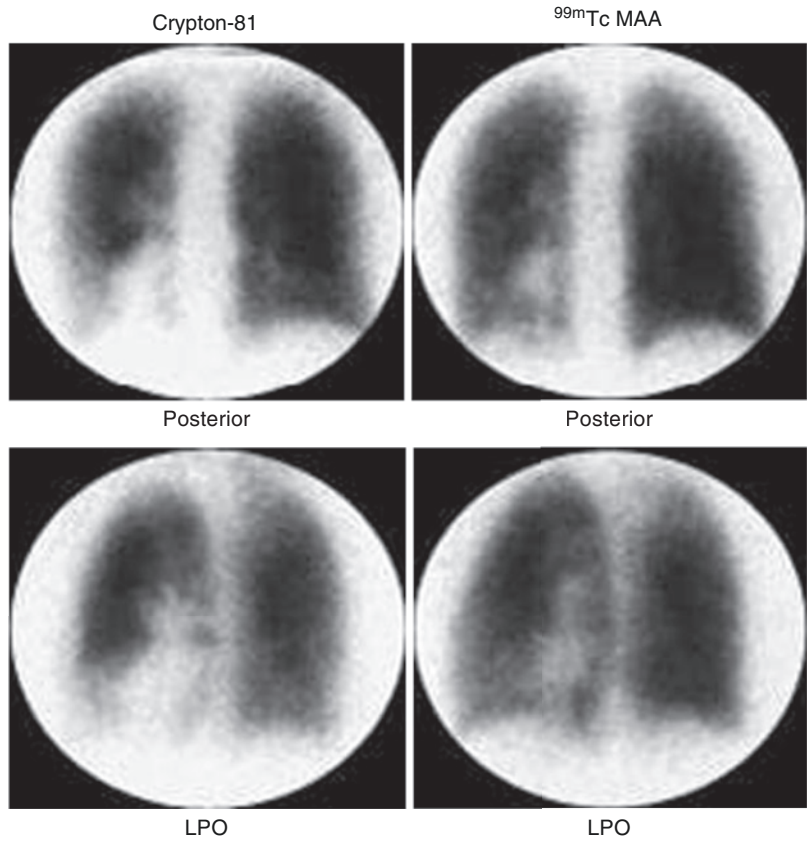
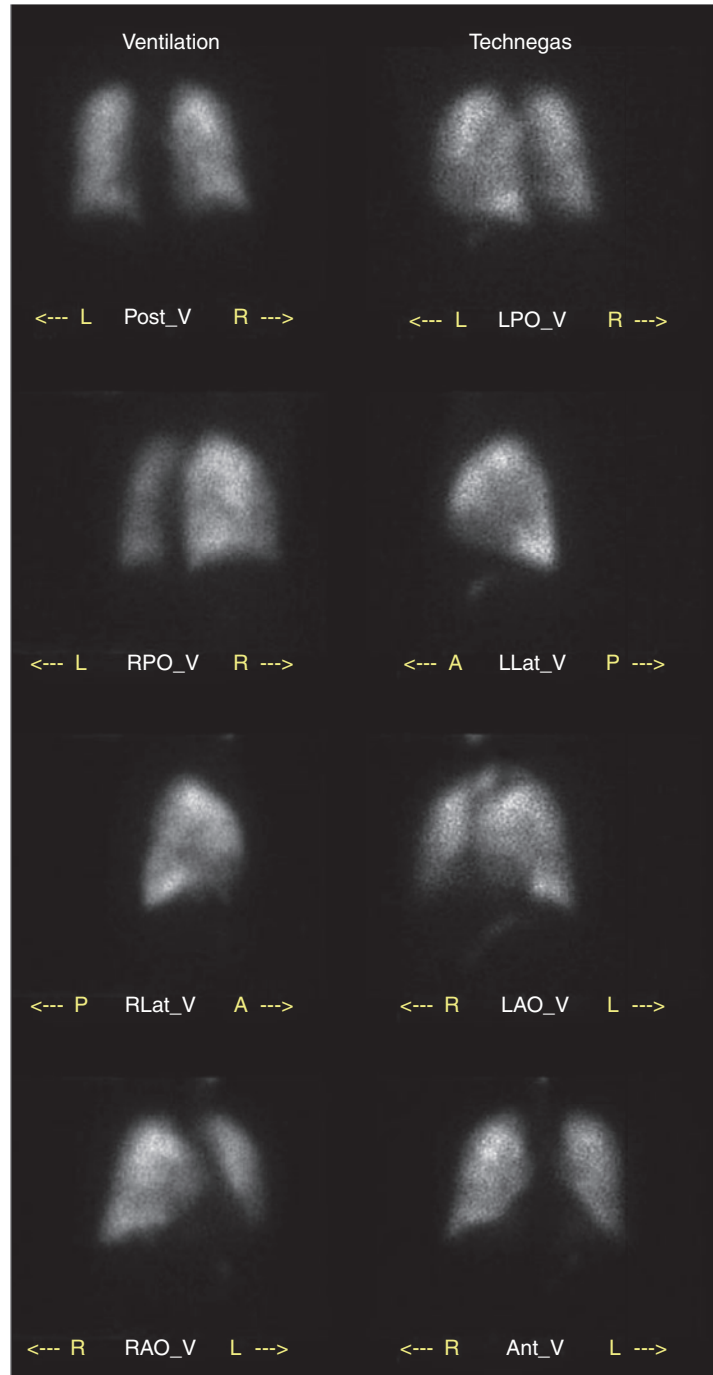


Fig. 8.10 ^{99m}Tc-DTPA aerosol ventilation study. Images show no abnormalities. Observe the activity in the esophagus and stomach due to swallowed activity

Fig. 8.11 ^{99m}Tc -Technegas ventilation study for a patient suspected of having pulmonary embolism. The study shows no abnormalities and illustrates the good quality of ventilation studies obtained using this agent. The perfusion, on the other hand, reveals perfusion defects in both lungs and no matching ventilation or X-ray abnormalities, indicating a high probability of pulmonary embolism



camera with a low-energy general-purpose collimator. The typical radiation exposure to the lungs is about 100 mrad. This is less than the several hundred milli-rads exposure from a typical Xe133 rebreathing ventilation exam. The dose to the lungs is also less than that from a Kr-81. Images

should be acquired for 100 K counts or 5 min. Exposure to personnel is usually less than that delivered a Xenon study.

Technegas is a ventilation aerosol agent that gained popularity recently. It is ultrafine labeled carbon particles produced by heating ^{99m}Tc -

perchnetate to very high temperatures of approximately 2500 °C in the presence of 100% argon gas. An ash material is produced that acts like a gas with good peripheral deposition because the particles are so small, with a median size of 0.05–0.15 µm. Technegas has a half-clearance time of 4–6 h. Since the material produced is not filtered and contains up to 50% of the initial radioactivity, a large number of appropriately sized particles are inhaled with each breath. Thus, only a few inspirations (typically 2–10) are needed to reach an adequate dose. Usually about 1 mCi is deposited in the lung. Extrapulmonary activity in the oropharynx, trachea, and stomach can be seen in about 30% of patients. The exam may be technically inadequate in up to 15% of patients particularly in severely ill patients that cannot be instructed for inhalation or in patients with very shallow or rapid breathing. If the Technegas portion of the exam is performed following the perfusion study, a counting rate of at least two times the count rate of the perfusion exam is considered adequate.

Another agent, perchnetegas, which is a vapor of perchnetate, is prepared similarly but, in the presence of 2–5% oxygen, has a shorter clearance time and shows excellent deposition in the lungs. Table 8.4 summarizes the essential information relevant to its use in obtaining adequate perfusion scan.

Table 8.4 Characteristics of ^{99m}Tc -macroaggregated albumin (^{99m}Tc -MAA)

Size	10–90 µm (mostly 20–50)
Minimum number of particles to be used in adults	100,000 unless pulmonary hypertension or right to left shunt is present
Ideal number of particles	200,000–500,000
Biologic half-life	4–8 h
Injection	Slow intravenous. Care should be taken not to cause particle aggregates that can produce hot spots
Safety	Particles block <1/1000 of the capillaries and precapillary arterioles

Interpretation of V/Q Scan

For proper interpretation of lung perfusion/ventilation study, chest X-ray must be available and should be obtained within 12 h of the time of the scans.

Normal perfusion study (Fig. 8.12) rules out any clinically significant pulmonary emboli. Since the ventilation and perfusion lung scans lack specificity (Table 8.5), probabilities have been used for the interpretation of abnormal studies. Based on the pathophysiological changes and scintigraphic observations, several scintigraphic features of perfusion abnormalities are known to affect the probability of a scan for pulmonary emboli (Table 8.6). One of the important features is the size of segmental perfusion defects. A small defect occupies up to 25% of the segment, a moderate defect between 25 and 75%, while a large defect takes up 75% or more. Using these features, several retrospective and prospective studies were conducted to refine the interpretation of ventilation and perfusion scans and assess their value in managing patients suspected of having embolic disease [67–71]. PIOPED study [32] established the value of normal and high-probability scans in excluding and diagnosing pulmonary embolism. It validated the segment equivalent concept (Fig. 8.13) and clarified the use of Bayesian analysis utilizing the clinical pre-scan and scan probabilities to figure the post-scan or diagnostic probability. The study showed clearly that when the clinical odds agree with the scan probability in the low- and high-probability categories, pulmonary embolism can be ruled out or confirmed with a high degree of certainty.

Based on the modifications of PIOPED criteria and other validated criteria, a simplified set is shown in Table 8.7. Small perfusion defects indicate low probability of pulmonary emboli as well as matching perfusion and ventilation defects regardless of size with no matching X-ray abnormalities (Fig. 8.14). Nonsegmental defects also indicate low probability. When perfusion defects match the X-ray abnormalities, it may indicate low, intermediate, or high probability based on the relative size of perfusion compared to the X-ray densities. When the perfusion defect is of

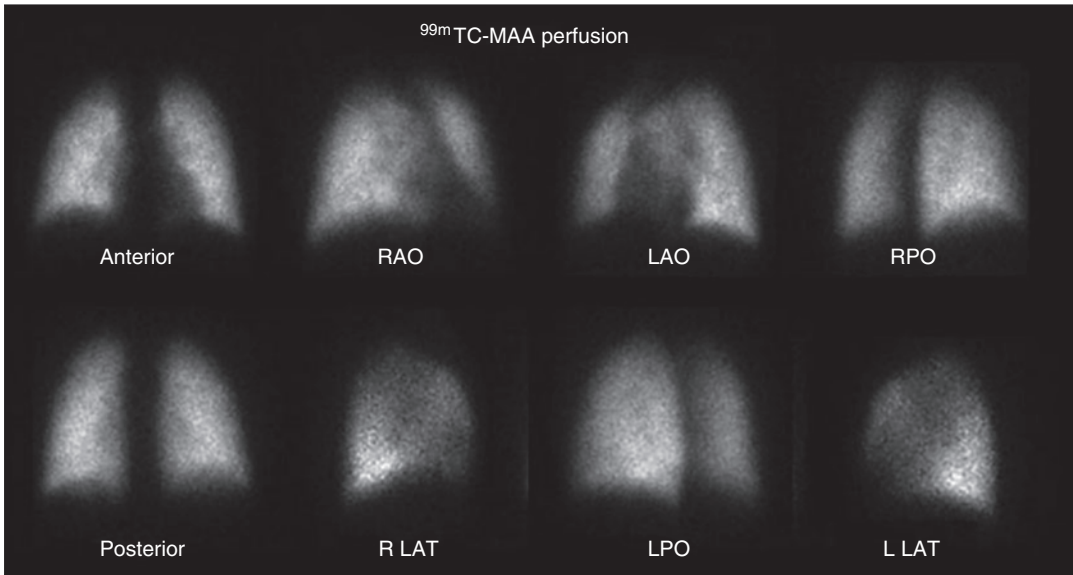


Fig. 8.12 Normal perfusion study. A ^{99m}Tc-MAA perfusion scan of a patient suspected of having pulmonary embolism. The perfusion study reveals uniform perfusion

throughout both lungs with no defects. Note the parallel medial borders of both lungs on the posterior view and the sharp delineation of the costophrenic angles

Table 8.5 Causes of abnormal perfusion lung scintigraphy

Emphysema
Inflammatory diseases
Pneumonia
Abscess
Granulomatous disease (sarcoidosis, tuberculosis)
Pulmonary fibrosis
Bronchial obstruction
Infection
Neoplasm
Acute and chronic asthma
Mucus plug
Foreign body
Rib fractures (reduced lung excursion)
Congenital hypoplasia or absence of the pulmonary arteries
Peripheral pulmonary artery stenosis
Thromboembolic disease
Thrombus
Tumor embolism
Fat embolism
Air embolism
Extrinsic vessel compression (tumor, inflammation)
Left ventricular failure
Mitral valve disease
Veno-occlusive disease
Prior lung resection
Radiation

Table 8.6 Features of perfusion defects associated with higher probability of pulmonary emboli

Size	Moderate and large
Larger relative size compared with that of chest X-ray densities	
Location	Pleural-based defects
Lower lobes	
Shape	Wedge shaped
Type	Segmental
Relation to ventilation pattern	Mismatching
Number	Multiple

the same approximate size of the matching X-ray density (Fig. 8.15), it indicates intermediate probability (approximately 25%).

The minimum number of mismatching perfusion defects is two segment equivalent defects with no matching chest X-ray abnormalities to make a high-probability interpretation (Fig. 8.16). However, a study analyzing PIOPED data indicated that defects equivalent of 1.5 segments are indicating high probability among patients with no prior cardiopulmonary diseases [72].

To improve interpretation, SPECT is being used more frequently in V/Q scans. SPECT scintigraphy has been reported to be strongly preferred to V/Q planar as it provides more accurate

Fig. 8.13 The segment equivalent concept. (From Morpurgo and Schmid [39] with permission)

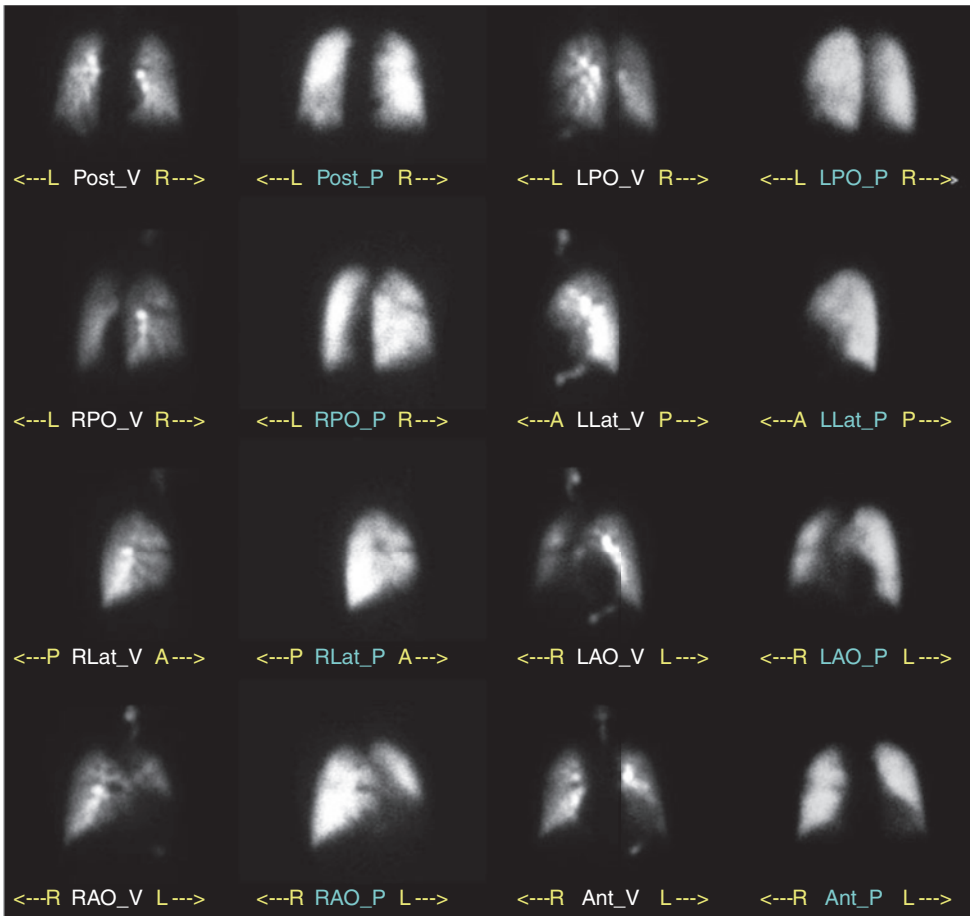
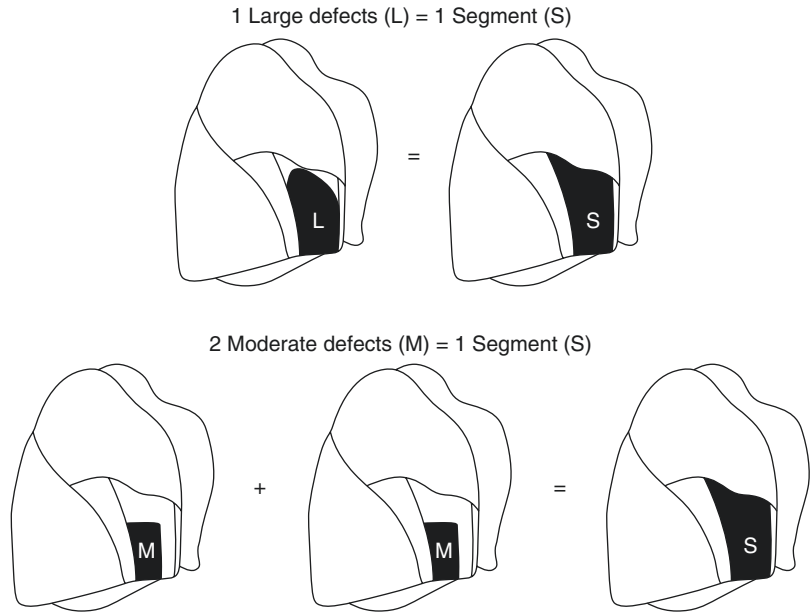


Fig. 8.14 ^{99m}Tc-DTPA aerosol ventilation and ^{99m}Tc-MAA perfusion studies of a patient suspected of having pulmonary embolism. The X-ray was normal. The per-

fusion study shows multiple small perfusion defects matching the ventilation pattern indicating low probability of pulmonary emboli

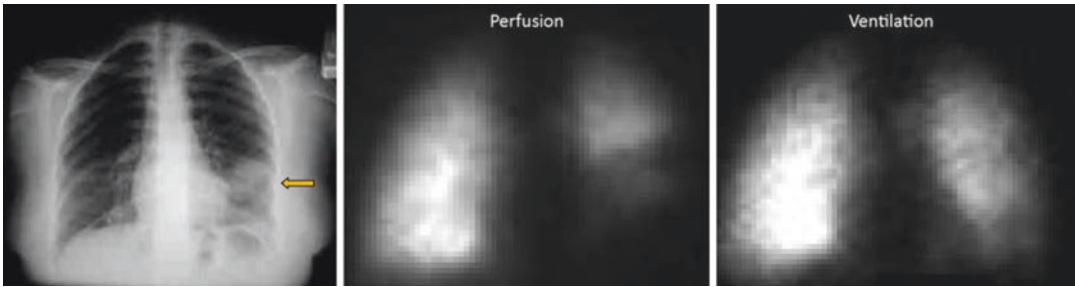


Fig. 8.15 Chest X-ray of a patient referred to rule out pulmonary embolism with a density in the left lower lobe (arrow) matching the perfusion defect on ^{99m}Tc -MAA

scan and is of the same approximate size indicating intermediate probability of pulmonary emboli

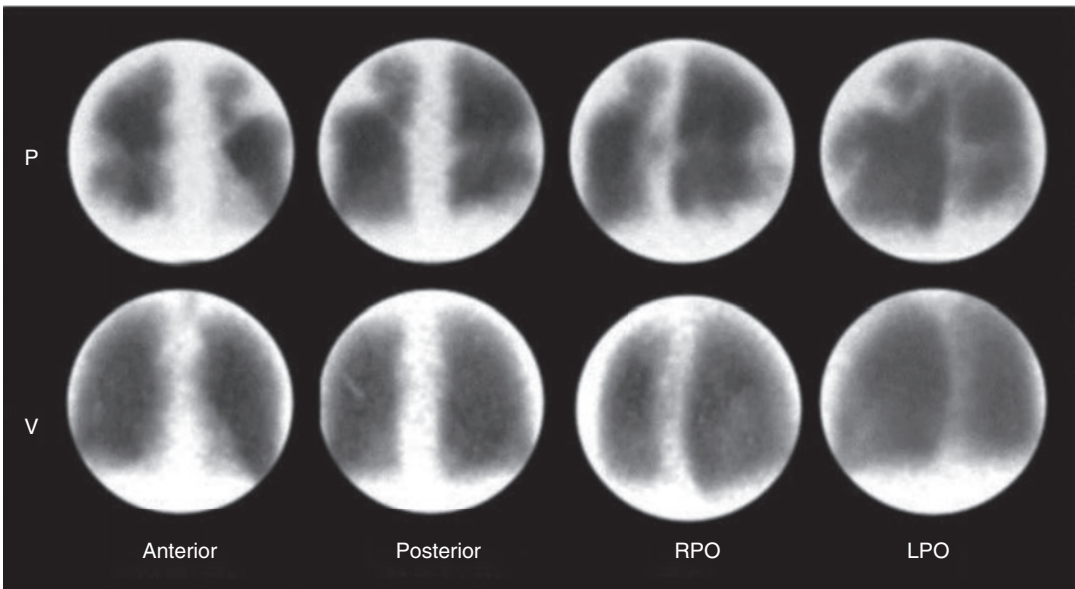


Fig. 8.16 Ventilation and perfusion scans of a 74-year-old man with history of fracture of left femur 3 days earlier treated with internal fixation. Patient was referred to rule out pulmonary emboli because of acute onset of shortening of breath. Perfusion study shows multiple per-

fusion defects equivalent to more than two segments with no matching abnormalities on ventilation study and no corresponding changes in the chest X-ray which was normal. This illustrates a typical pattern of high probability of pulmonary emboli on ventilation/perfusions scans

diagnosis of PE even in the presence of comorbid diseases such as COPD and pneumonia [64, 65, 73, 74].

Recently, trinary interpretative system for V/Q scans has been proposed and validated in some studies. This system is similar to the interpretative strategy for CT. V/Q scans were interpreted as “PE present,” “PE absent,” or “nondiagnostic.” According to this system, the normal, very low (near normal), and low probabilities are grouped

together and reported as PE absent. The high-probability pattern is reported as PE present, while the intermediate patterns are reported as nondiagnostic [75].

This approach can simplify the scan report for the referring physicians since the probability system still causes confusion. This leads to decrease in the utilization of V/Q scans although recent data show increasing evidence that lung scintigraphy is not only safe but also accurate enough to

Table 8.7 Criteria for the interpretation of ventilation/perfusion lung scans

Category	Pattern on V/Q images
Normal	No perfusion defects. Allow for impressions explained by enlarged heart or other hilar structures as seen on chest X-ray
Near normal	Nonuniform uptake with no definite segmental or subsegmental perfusion defects
Low	Nonsegmental perfusion defects other than those explained by cardiomegaly or other prominent hilar structures
	Matching V/Q defects with no corresponding CXR abnormalities
	Any number of only small defects regardless of ventilation and CXR patterns
	Stripe sign
High	Perfusion defect substantially smaller than CXR abnormality
	Two or more large mismatching defects or their equivalent (4 moderate or 1 large plus 2 moderate defects) with no corresponding CXR abnormalities
	Perfusion defect substantially larger than CXR abnormality ^a
Intermediate	Perfusion defect matching chest X-ray abnormality and of the same approximate size.
	Single moderate up to less than two segmental mismatching defects with no corresponding chest X-ray abnormalities
	Difficult to categorize as low or high

^a 1.5 in patients with no prior cardiopulmonary disease can be considered high probability

be quite useful clinically in patients with suspected PE. It is available conveniently in the clinical setting. Additionally, using the scintigraphic diagnostic strategy results in an important reduction of radiation dose, particularly for the female breast [76].

Many algorithms have been developed to diagnose PE utilizing D-dimer test, echo cardiography, Doppler ultrasound, scintigraphy, and multislice CT. None of these algorithms have gained uniform acceptance, and many variations were found in practice patterns among physicians, geographic locations, available resources, and experience [77].

Till further development, proper utilization of V/Q scans along with the DVT imaging and laboratory tests and CT solves most diagnostic problems and minimizes the need for angiograms (Table 8.7) [78].

8.3 Pulmonary Hypertension

Normal pulmonary artery systolic pressure at rest is 18–25 mmHg, with a mean pulmonary pressure ranging from 12 to 16 mmHg. This low pressure is due to the large cross-sectional area of the pulmonary circulation, which results in low resistance. An increase in pulmonary vascular resis-

tance or pulmonary blood flow results in pulmonary hypertension. It is defined as a pulmonary artery systolic pressure higher than 30 mmHg or a pulmonary artery mean pressure higher than 20 mmHg.

Pulmonary hypertension may have no cause (primary) which is rare or may follow cardiac or pulmonary disorders (secondary). Pathophysiologically, three predominant mechanisms may be involved in the pathogenesis of secondary pulmonary hypertension, (1) hypoxic vasoconstriction, (2) decreased area of the pulmonary vascular bed, and (3) volume/pressure overload.

Chronic hypoxemia such as due to COPD causes pulmonary vasoconstriction by a variety of actions on pulmonary artery endothelium and smooth muscle cells.

A variety of causes may decrease the cross-sectional area of the pulmonary vascular bed, primarily due to disease of the lung parenchyma. Examples of these conditions include collagen vascular diseases particularly systemic scleroderma or CREST (calcinosis cutis, Raynaud phenomenon, esophageal motility disorder, sclerodactyly, and telangiectasia) syndrome and acute and chronic pulmonary emboli [29, 30].

Disorders of the left heart may cause secondary pulmonary hypertension, resulting from volume and pressure overload. Pulmonary blood

volume overload is caused by left-to-right intracardiac shunts, such as in patients with atrial or ventricular septal defects. Left atrial hypertension causes a passive rise in pulmonary arterial systolic pressure in order to maintain a driving force across the vasculature.

8.4 *Pneumocystis carinii* (jiroveci) Pneumonia

Pneumocystis carinii (jiroveci) is an opportunistic pathogen currently classified as a fungus [79]. It is a significant cause of morbidity and mortality in human immunodeficiency virus and nonhuman immunodeficiency virus-associated immunosuppressed patients [80, 81] although it also occurs in non-immunocompromised patients [82–85]. Highly effective active antiretroviral therapy in industrialized nations however has led to dramatic declines in the incidence of AIDS-associated complications, including PCP, but no decline has occurred in the developing countries [80, 81]. The organism attaches to the alveolar macrophages through a mechanism that involves fibronectin. The trophozoite develops into cysts that produce daughter trophozoites. As the number of organisms increase, the permeability of the alveolar capillary endothelium increases, producing respiratory distress. Typically, infection with *P. carinii* (now called *P. jiroveci*) produces a patchy or lobar interstitial pneumonia or, rarely, a bronchopneumonia pattern. Severe infections produce diffuse alveolar damage. The classical histological findings consist of alveolar exudates having a granular or foamy appearance that represent nonstaining clusters of the cysts and trophozoites of *P. carinii* within an eosinophilic staining background of the organism's filopodia and host cellular debris. Atypical pulmonary reactions include the formation of granulomas, focal pulmonary infection, and cavitory lesions. In extremely immunosuppressed persons, the inflammatory reaction may be minimal and consist only of sparse collections of alveolar macrophages. Since clinical manifestations of *P. carinii* pneumonia (PCP) in AIDS patients may precede X-ray changes by at least 2 weeks and as long as

18 months, ^{67}Ga has an important role in the diagnosis of early PCP. ^{67}Ga is more sensitive than chest X-ray for early PCP and is more accurate in measuring the extent of inflammation. The pattern of uptake is typically diffuse and bilateral (Fig. 8.17), although other patterns may be noted [84, 85]. Localized lung uptake and perihilar uptake patterns can be seen in addition to the diffuse pattern, which may be further classified into homogeneous and heterogeneous diffuse patterns. The heterogeneous pattern has the highest positive predictive value, which is even more specific when it is of high-grade uptake and when accompanied by normal chest radiograph.

8.5 Idiopathic Pulmonary Fibrosis

Idiopathic pulmonary fibrosis is a rare disease characterized by chronic, progressive irreversible interstitial lung fibrosis along with inflammatory changes of unknown cause. Clinically, the condition is often diagnosed at an advanced stage, carry a poor prognosis. The median estimated survival time from the time of diagnosis is 2–5 years. Recently several subtypes have been clearly identified with different outcomes [86, 87]. Idiopathic pulmonary fibrosis is characterized by parenchymal inflammation and interstitial fibrosis that may eventually be fatal. The inciting factors in the development of IPF remain unknown. A widely held hypothesis is that this disorder occurs in susceptible individuals following some unknown stimuli. The inciting agent initiates a cascade of events that involve factors controlling inflammatory, immune, and fibrotic processes in the lung. Viral, immunological, and genetic (supported by finding familial cases) factors appear to play an important role [87]. The main feature in IPF is alveolitis, which is chronic inflammation of the alveolar unit followed by fibrosis. The destruction is mediated by inflammatory (neutrophils and macrophages) and immune (immune complex disease) processes, where immune effector cells injure lung cells and induce connective tissue proliferation. The chronic active inflammation is important and

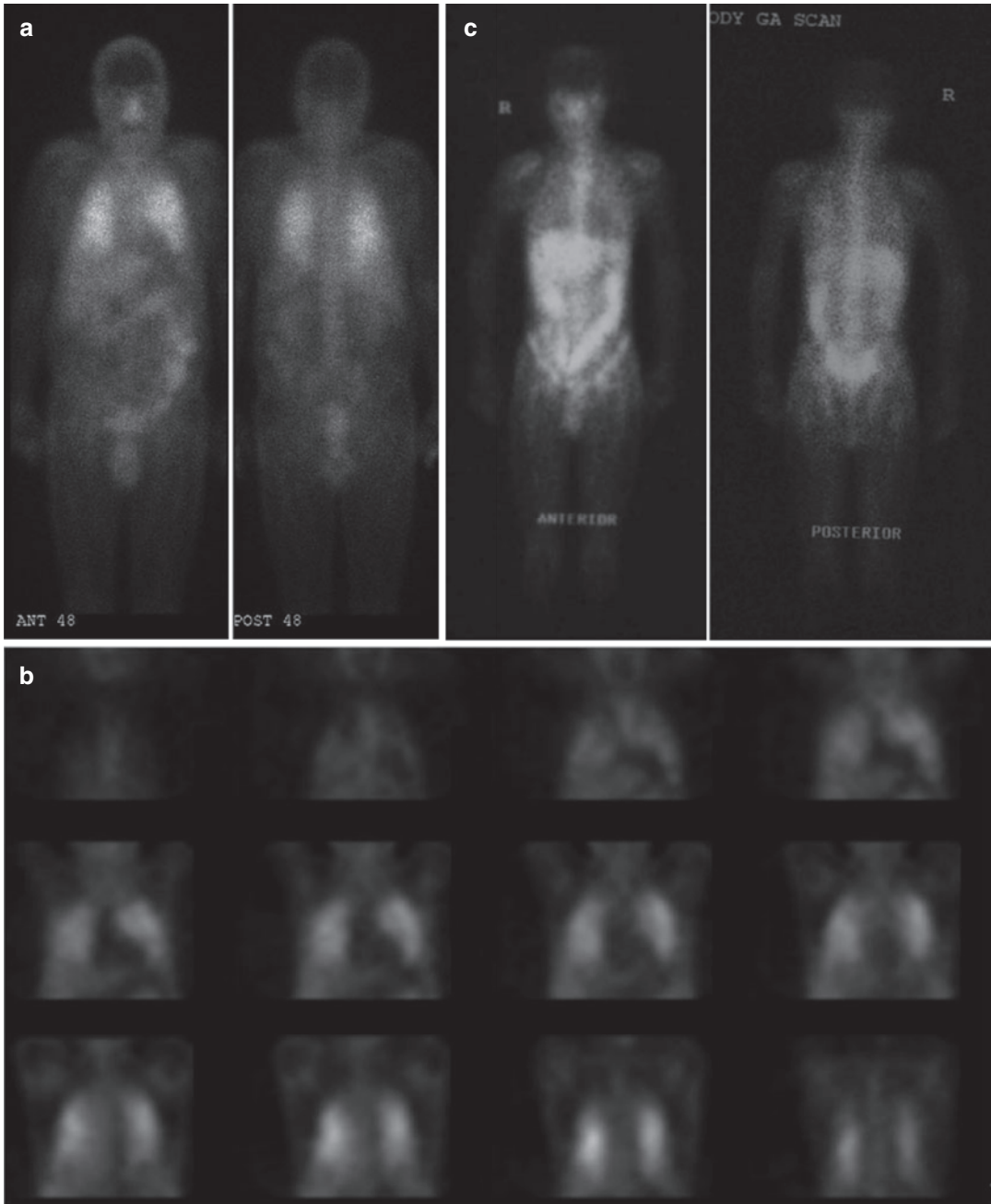


Fig. 8.17 (a–c) Gallium-67 images of two AIDS patients with PCP obtained 48 h post-injection. Planar (a) and SPECT (b) of one patient show significantly increased accumulation of the radiotracer illustrating severe infec-

tion. Planar image of the other patient (c) shows slightly increased accumulation of the radiotracer in both lungs diffusely illustrating mild form of PCP infection

directs the investigations for diagnosis. The fibrotic and destructive changes distort the normal lung architecture and result in morbidity.

The major histopathological findings vary from active alveolitis and minimal fibrosis in early cases to severe fibrosis and honeycombing with minimal alveolitis in late stages. The alveolitis is characterized by an outpouring of mononuclear cells, macrophages, and lymphocytes into the alveolar space, with relatively intact alveolar walls which will be deranged by edema, fibrinous exudate, mononuclear cell infiltration, and fibroblast proliferation [86]. Connective tissue alteration occurs later in the process. Recent classification of the type of fibrosis depends on the predominant cell type. Patients with more cellular findings respond to treatment favorably and have a better long-term prognosis compared with those with more fibrotic changes. ^{67}Ga has an important role in evaluating the activity of the disease and in following up the response to treatment. The degree of ^{67}Ga uptake correlates with the degree of interstitial and alveolar cellularity as seen on lung biopsies. Accordingly, it helps evaluate the extent and activity of the disease by visual assessment and/or quantitation of the uptake [88].

8.6 Pulmonary Sarcoidosis

Sarcoidosis, a multisystem granulomatous disorder, occurs most commonly in young adults, more commonly in blacks and in temperate areas. A second peak is known to occur in older age group (over age 60) [89]. The exact etiology of the disease is unknown, but it is believed to be due to exaggerated cellular immune response on the part of helper/inducer T lymphocytes to exogenous or autoantigens. It presents most frequently as bilateral hilar adenopathy, pulmonary infiltrates, and skin and eye lesions. It may be acute or chronic. Current evidence points to genetic predisposition and exposure to yet unknown transmissible agent(s) and/or environmental factors as etiological agents. Recently it has been recognized to be a Th1 mediated disease as it is

dominated by gene signatures associated with $\text{IFN}\gamma$ signaling [90, 91].

The acute variant has an abrupt onset and may commonly show spontaneous remission within 2 years; the response to steroids is excellent. The chronic variant has an insidious onset and is more likely to cause progressive disease with fibrosis. The disorder is characterized by the presence of epithelioid (correct spelling) granuloma in affected organs that may lead to fibrosis and organ dysfunction. Granulomas of sarcoidosis often exist diffusely throughout the body despite the lack of clinical evidence of disease. Histological features are usually quite typical, but not specific. The architecture of the lesion is that of multiple similar granulomas, consisting of whorls of elongated cells (fibroblasts and epithelioid cells) with mononuclear inflammatory cells at their periphery. Giant cells are located within the granulomas (Fig. 8.18), and multinucleated cellular inclusion bodies are frequently found. Scarring with fibrosis suggests chronicity. Epithelioid cells secrete a number of cytokines and other mediators including angiotensin-converting enzyme (ACE) which is suggested to reflect the granuloma burden in sarcoidosis and may play a role in its pathophysiology. Lung is involved in more than 90% of cases. Pulmonary sarcoidosis starts as diffuse interstitial alveolitis, followed by the characteristic granulomas. Granulomas are present in the alve-

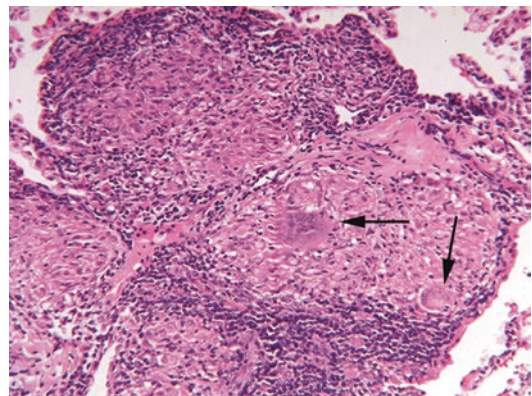


Fig. 8.18 Microphotograph of a noncaseating granuloma of a case of sarcoidosis. Note multinucleated giant cells (arrows)

olar septa as well as in the walls of the bronchi and pulmonary arteries and veins. The center of the granuloma contains epithelioid cells derived from mononuclear phagocytes, multinucleated giant cells, and macrophages. Lymphocytes, macrophages, monocytes, and fibroblasts are present at the periphery of the granuloma [92]. Sarcoidosis represents a challenge to clinical investigation because of its unpredictable course, uncertain response to therapy, and diversity of potential organ involvement and clinical presentations [93].

The diagnosis is based on a compatible clinical and/or radiologic picture, histopathological evidence of noncaseating granulomas in tissue biopsy specimens, and exclusion of other diseases capable of producing similar clinical or histopathological appearances [59]. Patients with pulmonary sarcoidosis may have no symptoms and are discovered by chest X-ray obtained

for nonpulmonary reasons. When symptomatic, dyspnea, chest pain, and cough are the most common chest symptoms [93]. For many years, pulmonary sarcoidosis has been staged into four stages (Table 8.8) based on chest X-ray findings [94]. The distinction between sarcoidosis and tuberculosis can be difficult at times, and the two diseases may coexist in the same patient. Similar granulomas may occur in a wide variety of other diseases, such as with malignancy or immune deficiencies, berylliosis, and foreign body reactions. ^{67}Ga is useful in evaluating the activity of the disease and the response to therapy. Semiquantitative and quantitative methods of grading ^{67}Ga uptake can be helpful. Diffuse lung uptake and bilateral hilar uptake (Fig. 8.19) are the most common patterns seen, but they lack specificity [94]. The major value of ^{67}Ga is in evaluating the activity of the disease, in detecting extrathoracic sites of involvement, and in evaluating the response to therapy. Ventilation and perfusion scans do not have a specific role in sarcoidosis. However, it should be known that a mismatching pattern is among those seen in the disease and can be falsely interpreted as indicating a high probability of pulmonary emboli.

Table 8.8 Radiologic staging of pulmonary sarcoidosis

Stage 1	Hilar adenopathy alone
Stage 2	Adenopathy plus infiltrates
Stage 3	Infiltrates only
Stage 4	Fibrosis

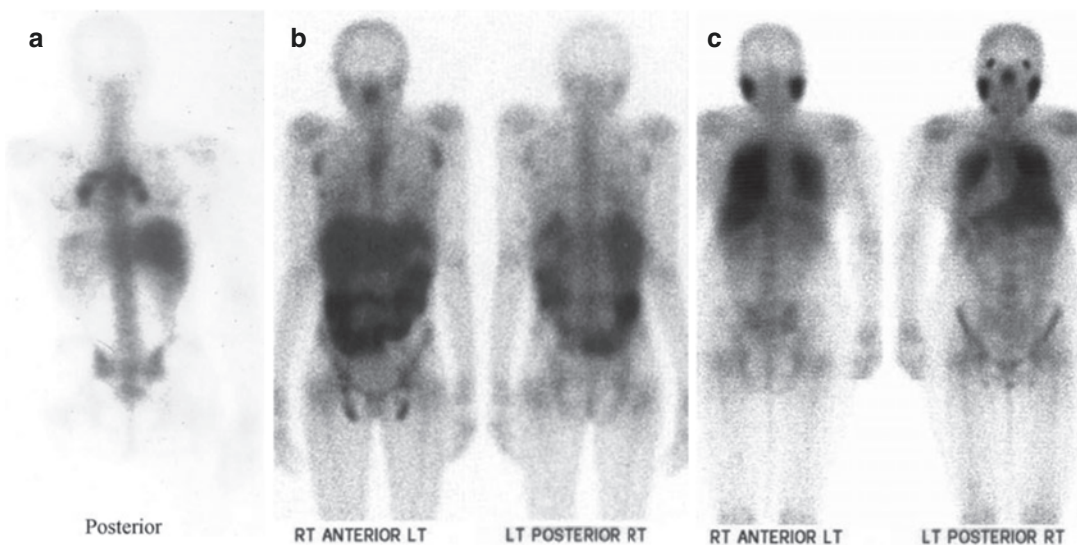


Fig. 8.19 Forty-eight-hour Ga-67 posterior image of a patient with sarcoidosis showing uptake in the hilar nodes bilaterally (a). Another patient's study is shown (b) Ga-67 images for a patient with sarcoidosis illustrating uptake in

the axillary and inguinal lymph nodes as well as mild diffuse accumulation in the lungs and (c) a patient with diffuse lung uptake and intense uptake in the parotids and lacrimal gland

FDG uptake in sarcoidosis (Fig. 8.20) is nonspecific in both intensity and pattern and is not generally useful in making an initial diagnosis. FDG uptake can decrease when sarcoidosis is treated, and PET can be useful in monitoring the effectiveness of therapy. Accordingly, PET/CT can be useful in monitoring disease progression or remission [95].

8.7 Obstructive Airway Disease

Chronic bronchitis, emphysema, and bronchial asthma are collectively known as obstructive airway disease. Chronic bronchitis and emphysema are common among smokers but are also caused by air pollutants. In chronic bronchitis, the walls of the bronchi and bronchioles are inflamed with edema, cellular infiltrates, fibrosis, and an increase in the mucus glands and bronchial secretions and thickening of the bronchial walls. All these changes result in progressive narrowing of the lumina of the bronchi and bronchioles.

Emphysema indicates irreversible dilation of the alveoli, and destruction of their septa can occur alone or, commonly, in association with chronic bronchitis as part of chronic obstructive airway disease. Hyperinflation of the alveoli and septal destruction may lead to formation of large air spaces (bullae). Air spaces formed adjacent to the pleura are called blebs. There are three types of emphysema:

1. In centrilobular emphysema, the central areas of the lungs are affected by alveolar dilation. This type is most commonly associated with chronic bronchitis in smokers. It affects more the upper lobes and usually spares the alveoli.
2. Panlobular emphysema involves an entire lobe with randomly distributed damage. It involves more the lower lobes of the lungs, older individuals, and patients with alpha 1 antitrypsin deficiency.
3. Localized (previously paraseptal) emphysema is characterized by emphysematous changes in only one or at most a few locations, with the remainder of the lung normal. It is usually

F-18 FDG

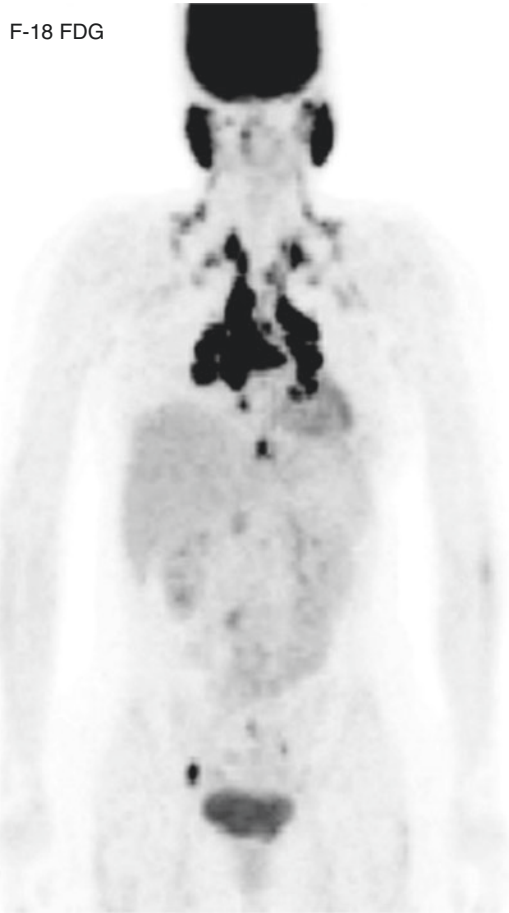


Fig. 8.20 F-18 FDG image of a 35-year-old female with proven sarcoidosis. The study shows uptake in the areas of active inflammation in mediastinum, pulmonary hilus, salivary glands, and cervical, supraclavicular, axillary, para-aortic, iliac, and inguinal lymph nodes. (Courtesy of Professor Osama Sabry)

of no clinical significance; however, the rather common subpleural bullae may rupture and cause spontaneous pneumothorax.

Bronchial asthma is characterized by episodes of airflow obstruction, which affect both large and small airways. Decreased ventilation and perfusion can be seen on ventilation and perfusion scans within moments of the asthma attack.

Obstructive airway disease can cause an abnormal ventilation scan with or without abnormal perfusion. Xenon-133 is the most sensitive agent for detecting the ventilation abnormalities, particularly in the washout phase. ^{99m}Tc -DTPA aerosol

studies show nonuniformity with varying degrees of central deposition of the particles, depending on the severity of bronchial narrowing (Fig. 8.21). The associated perfusion abnormalities range from minimal nonuniformity to complete absence of perfusion, matching the ventilation defects. Obstructive airway disease is commonly seen among patients suspected of having pulmonary emboli. This may pose difficulty in interpreting the ventilation and perfusion images to establish whether a matching pattern is present [96], but the same criteria of interpretation are applied to determine the probability of pulmonary emboli as in patients with no obstructive airway disease.

8.8 Pleural Effusions

Many etiologies can cause pleural effusion, including inflammatory, traumatic, and neoplastic diseases, and disturbance in organ functions. Pulmonary embolism is not uncommonly associated with pleural effusion. Based on the underlying cause, pleural effusion may consist of transudate, exudate, pus, or blood. With pleural effusions, there is diminished ventilation and perfusion, which is proportional to the amount of effusion [97]. Elevated hemidiaphragm causes a similar pattern. The appearance of pleural effusion may change with the position of the patient

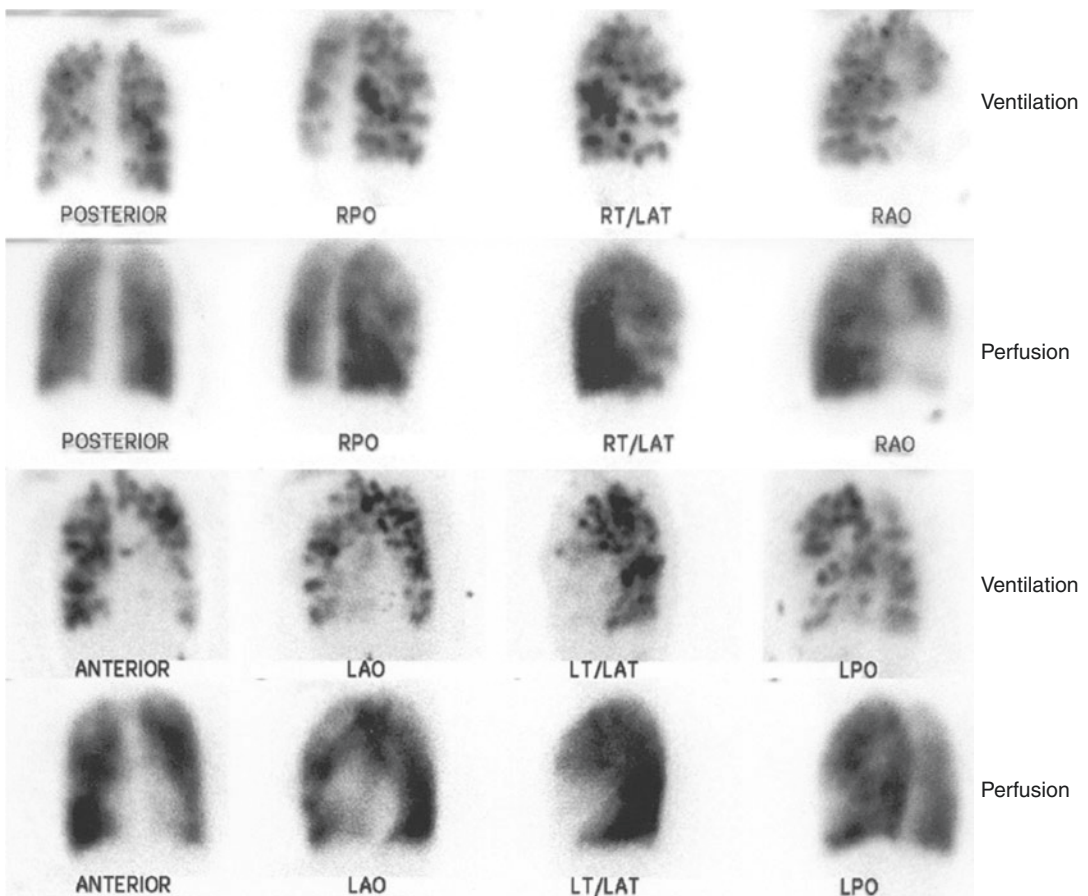


Fig. 8.21 ^{99m}Tc -DTPA aerosol image of a patient with severe obstructive airway disease. Note the central deposition of the radiotracer at the sites of the narrowed openings of the bronchi and bronchioles

when effusion is freely mobile or may not change when the effusion is loculated or encapsulated.

8.9 Pneumonia

Pneumonia is an acute inflammation of the lung parenchyma, which often impairs gas exchange. The condition is prevalent in infants, old individuals, and immunocompromised patients. It is the leading secondary cause of death in the USA. Three major types can be recognized: lobar, lobular (bronchopneumonia), and interstitial. Lobar pneumonia is usually bacterial and involves the alveoli of one lobe or more, but not the bronchi. Chest X-ray and other imaging modalities show varying degrees of abnormalities based on the amount of inflammatory exudate. X-ray will show opacities of different degrees, while nuclear medicine procedures such as labeled WBC or ^{67}Ga (Fig. 8.22) show abnormalities correlating in size and intensity with the

severity of inflammation and its duration (see Chap. 4). Lobular pneumonia (bronchopneumonia) shows inflammation of bronchi, bronchioles, and alveoli in a patchy manner. Interstitial pneumonia, also called pneumonitis or viral pneumonia, is a milder form that usually accompanies other viral conditions such as measles. Typically, no exudates are present in the alveoli.

8.10 Bronchial Obstruction

Bronchial obstruction may be caused by obstruction from within or from outside the bronchi. It may be acute, such as obstruction due to a foreign body or mucus plug, or gradual, as in some patients with bronchial compression by an adjacent mass. Depending on the level and severity of obstruction, the ventilation and perfusion are affected. Usually the ventilation is affected more severely than the perfusion and may be totally absent with complete obstruction (Fig. 8.23).

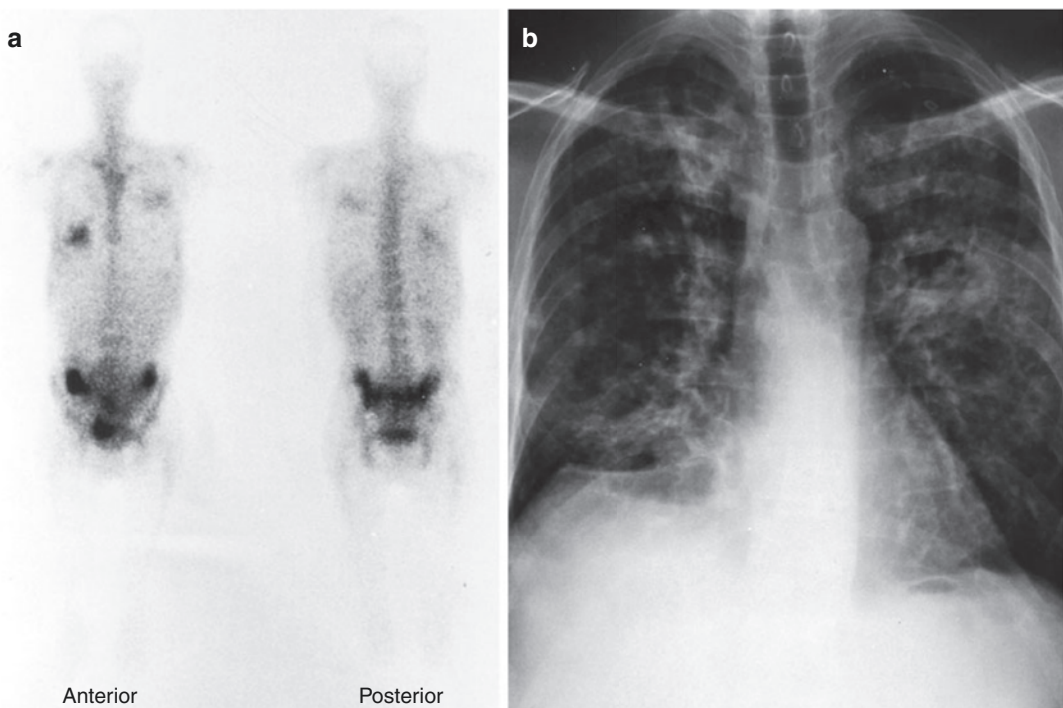


Fig. 8.22 Gallium-67 48-h study (a) shows two areas of increased accumulation of the radiotracer in the right lower and left mid lung zones in a patient with pneumonia. Chest X-ray (b) of the same patient shows infiltrates

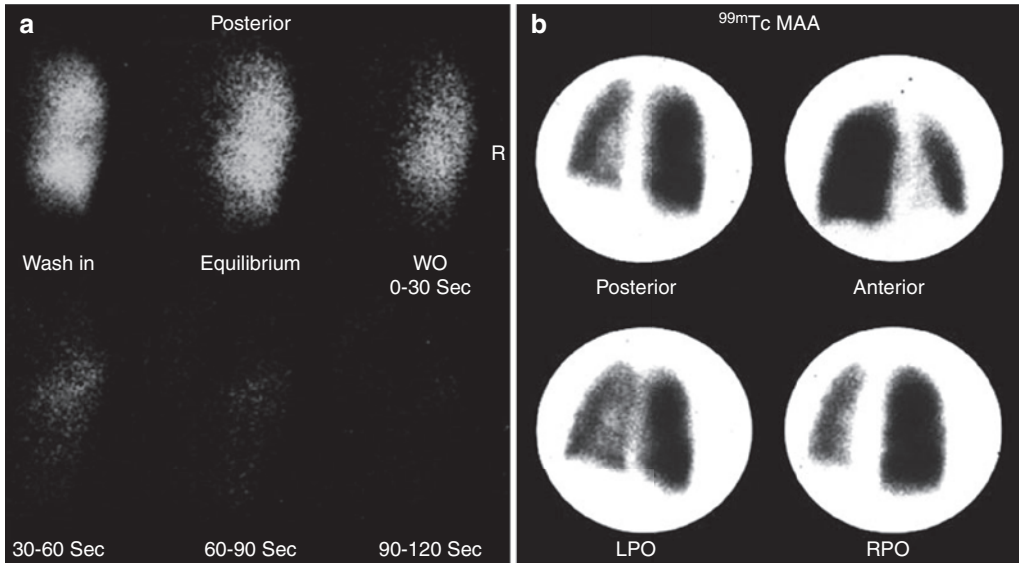


Fig. 8.23 (a, b) Xenon-133 washout images of a patient complaining of severe shortness of breath. The images reveal nonvisualized left lung. ^{99m}Tc -MAA perfusion study of the same patient shows decreased perfusion to

same lung diffusely. This pattern suggests bronchial obstruction with reflex vasoconstriction. The patient has a mucus plug obstructing the left main bronchus

8.11 Lung Cancer (See Chap. 12)

Lung cancer is the second most common cancer in both men and women (second to prostate and breast cancers). It is, however, the leading cause of cancer death in both men and women [98].

FDG-PET/CT is useful for imaging lung cancer since the tumor cells have both an increased uptake of glucose due to a higher number of Glut-1 surface proteins as well as a higher rate of glycolysis compared to nonneoplastic cells [99].

Histologically, lung cancer may be squamous (epidermoid), adenocarcinoma (bronchogenic carcinoma), small cell carcinoma, adenosquamous carcinoma, and anaplastic carcinoma. The role of nuclear medicine particularly PET/CT (Fig. 8.24) lies in the detection of the primary tumor in some patients, and more importantly staging of the tumor determines the best treatment choice, evaluating the response to therapy and sometimes predicting its success [100] (see Chap. 10). When pneumonectomy is planned for lung cancer, postoperative lung function can be predicted with optimal accuracy by a preoperative perfusion scan in the upright or supine positions. The ventilation scan is less accurate [101].

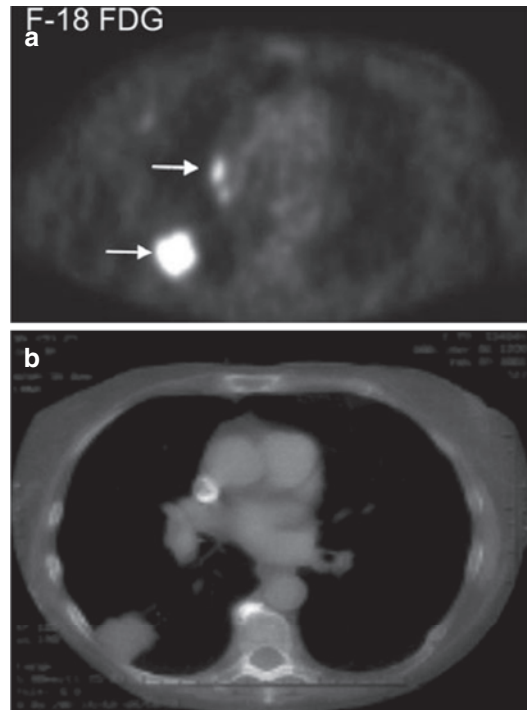


Fig. 8.24 (a, b) FDG-PET study illustrating right lung nodule with intense uptake and a mediastinal involvement (arrows) corresponding to lesions seen on CT scan. These represent non-small cell lung cancer. The example demonstrates the value of FDG in determining the nature of morphologic findings of nodules and in staging the disease

When pneumonectomy is planned for lung cancer, postoperative lung function can be predicted with optimal accuracy by a preoperative perfusion scan in the upright or supine positions. The ventilation scan is less accurate.

References

- Brashers BL, Davey SS (1998) Structure and function of the pulmonary system. In: McCance KL, Huether SE (eds) Pathophysiology, the biologic basis for disease in adults and children, 3rd edn. Mosby, St Louis, pp 1131–1157
- Thibodeau GA, Patton KI (1996) Anatomy and physiology, 3rd edn. Mosby, St Louis
- De Nardo GL, De Nardo SJ (1984) Thelungs. In: Freeman LM, Johnson PM (eds) Clinical radionuclide imaging, 3rd edn. Grune and Stratton, Orlando, pp 1051–1139
- Elgazzar AH (1997) Scintigraphic diagnosis of pulmonary embolism: unraveling the confusion seven years after PIOPED. In: Nuclear medicine annual. Lippincott, Raven, pp 69–101
- Raskob GE, Angchaisuksiri P, Blanco AN, Buller H, Gallus A, Hunt BJ, Hylek EM, Kakkar A, Konstantinides SV, McCumber M, Ozaki Y, Wendelboe A, Weitz JI (2014) Thrombosis: a major contributor to global disease burden. *Arterioscler Thromb Vasc Biol* 34:23632371
- Anderson FA Jr, Zayaruzny M, Heit JA, Fidan D, Cohen AT (2007) Estimated annual numbers of US acute-care hospital patients at risk for venous thromboembolism. *Am J Hematol* 82:777–782
- Turetz M, Sideris AT, Friedman OA, Tripathi N, Horowitz JM (2018) Pulmonary embolism: epidemiology, pathophysiology, and natural history of pulmonary embolism. In: Seminars in interventional radiology, vol 35, No. 2. Thieme Medical Publishers, New York, p 92
- Kucher N, Tapson VF, Goldhaber SZ, DVT FREE Steering Committee (2005) Risk factors associated with symptomatic pulmonary embolism in a large cohort of deep vein thrombosis patients. *Thromb Haemost* 93:494–498. <https://doi.org/10.1160/TH04-09-0587>. PMID: 15735800
- Stein PD, Matta F, Musani MH, Diaczok B (2010) Silent pulmonary embolism in patients with deep venous thrombosis: a systematic review. *Am J Med* 123(5):426–431
- Frieman DG, Suyemoto J, Wessler S (1965) Frequency of pulmonary thromboembolism in man. *N Engl J Med* 272:1278–1280
- McLachlin J, Patterson JC (1961) Some basic observations on venous thrombosis and pulmonary embolism. *Surg Gynecol Obstet* 93:1–8
- Moser KM (1990) Venous thromboembolism: state-of-the-art. *Am Rev Respir Dis* 141:235–249
- Muñoz FJ, Mismetti P, Poggio R et al (2008) Clinical outcome of patients with upper-extremity deep vein thrombosis: results from the RIETE Registry. *Chest* 133(1):143–148
- Palevsky HI, Alavi A (1991) Noninvasive strategy for management of patients suspected of pulmonary embolism. *Semin Nucl Med* 21:325–331
- Miesbach W, Makris M (2020) COVID-19: coagulopathy, risk of thrombosis, and the rationale for anticoagulation. *Clin Appl Thromb Hemost* 26:1076029620938149. <https://doi.org/10.1177/1076029620938149>. PMID: 32677459; PMCID: PMC7370334
- Kipshidze N, Dangas G, White CJ, Kipshidze N, Siddiqui F, Lattimer CR, Carter CA, Fareed J (2020) Viral coagulopathy in patients with COVID-19: treatment and care. *Clin Appl Thromb Hemost* 26:1076029620936776. <https://doi.org/10.1177/1076029620936776>
- Salabei JS, Fishman TJ, Asnake ZT, Ali A, Iyer UG, et al (2021). COVID-19 coagulopathy: current knowledge and guidelines on anticoagulation. *Heart Lung*; 50: 357–360
- Colling ME, Kanthi Y (2020) COVID-19-associated coagulopathy: an exploration of mechanisms. *Vasc Med* 25:471–478
- Malas MB, Naazie IN, Elsayed N, Mathlouthi A, Marmor R, Clary B (2020) Thromboembolism risk of COVID-19 is high and associated with a higher risk of mortality: a systematic review and meta-analysis. *EclinicalMedicine* 29–30:100639
- Akel T, Qaqa F, Abuarqoub A, Shamon F (2020) Pulmonary embolism: a complication of COVID 19 infection. *Thromb Res* 193:79–82
- Bělohávek J, Dytrch V, Linhart A (2013) Pulmonary embolism, part I: epidemiology, risk factors and risk stratification, pathophysiology, clinical presentation, diagnosis and nonthrombotic pulmonary embolism. *Exp Clin Cardiol* 18(2):129–138
- Kamel E, Mckee T, Calcagni M, Schmidt S, Markl S, Bischof Delaloye A (2005) Occult lung infarction may induce false interpretation of F19 FDG PET in primary staging of pulmonary malignancies. *Eur J Nucl Med Mol Imaging* 32:641–646
- Manny J, Hechtman HB (1985) Vasoactive humoral factors. In: Goldhaber SZ (ed) Pulmonary embolism and deep venous thrombosis. Saunders, Philadelphia, p 283
- Dass H, Hcekscher T, Anthonisen NR (1967) Regional pulmonary gas exchange in patients with pulmonary embolism. *Clin Sci* 33:355–364
- Smith R, Alderson PO (1987) Ventilation perfusion scintigraphy in pulmonary embolism in pulmonary nuclear medicine. In: Loken MK (ed) Pulmonary nuclear medicine. Appleton and Lange, Norwalk, pp 51–79
- Wolfe MW, Skibo LK, Goldhaber SZ (1993) Pulmonary embolic disease: diagnosis, pathophysiologic aspects and treatment with thrombolytic therapy. *Curr Probl Cardiol* XVIII:587–633

27. National Heart, Lung and Blood Institute (1970) Urokinase pulmonary embolism trial – phase I results. *JAMA* 214:2163–2172
28. National Heart, Lung and Blood Institute (1974) Urokinase pulmonary embolism trial – phase II results. *JAMA* 229:1606–1613
29. Elgazzar AH, Jobalia R, Subramanian P, Ryan J, Hughes JA (1994) Multiple ventilation and perfusion (V/Q) scans in patients with and without pulmonary emboli (PE). *J Nucl Med* 35:239
30. Klok FA, Mos IC, van Kralingen KW, Vahl JE, Huisman MV (2012) Chronic pulmonary embolism and pulmonary hypertension. *Semin Respir Crit Care Med* 33:199–204
31. Hoepfer MM, Mayer E, Simonneau G, Rubin LJ (2006) Chronic thromboembolic pulmonary hypertension. *Circulation* 110:2011–2020
32. PIOPED Investigators (1990) Value of the ventilation/perfusion scan in acute pulmonary embolism: results of the prospective investigation of pulmonary embolism diagnosis (PIOPED). *JAMA* 263:2753–2759
33. Carson JL, Kelley MA, Duff A, Weg JG, Fulkerson WJ, Palevsky HI, Schwartz JS, Thompson BT, Popovich J Jr, Hobbins TE et al (1992) The clinical course of pulmonary embolism. *N Engl J Med* 326:1240–1245
34. Schober B (1980) Do pulmonary emboli lodge preferentially in prior foci? *J Nucl Med* 21:659–661
35. Hoffman JM, Lee A, Grafton S, Bellamy P, Hawkins RA, Webner M (1994) Clinical signs and symptoms in pulmonary embolism. A reassessment. *Clin Nucl Med* 19:803–808
36. Stein PD, Terrin ML, Hales CA, Palevsky HI, Saltzman HA, Thompson BT, Weg JG (1991) Clinical, laboratory, roentgenographic, and electrocardiographic findings in patients with acute pulmonary embolism and no pre-existing cardiac or pulmonary disease. *Chest* 100:598–603
37. Stein PD, Henry JW (1997) Prevalence of acute pulmonary embolism in central and subsegmental pulmonary arteries and relation to probability interpretation of ventilation/perfusion lung scans. *Chest* 111:1246–1248
38. Morgenthaler TI, Ryu JH (1995) Clinical characteristics of fatal pulmonary embolism in a referral hospital. *Mayo Clin Proc* 70:417–424
39. Morpurgo M, Schmid C (1995) The spectrum of pulmonary embolism. Clinicopathologic correlations. *Chest* 107:18S–20S
40. Sperry KL, Key CR, Anderson RE (1990) Towards a population-based assessment of death due to pulmonary embolism in New Mexico. *Hum Pathol* 21:159–165
41. Karwinski B, Svendsen E (1989) Comparison of clinical and postmortem diagnosis of pulmonary embolism. *J Clin Pathol* 42:135–139
42. Gross JS, Neufeld RR, Libow LS, Gerber I, Rodstein M (1988) Autopsy study of the elderly institutionalized patient: review of 234 autopsies. *Arch Intern Med* 118:173–176
43. Dismuke SE, Wagner EH (1986) Pulmonary embolism as a cause of death. *JAMA* 225:2039–2042
44. Goldhaber SZ, Hennekens CH, Evans DA, Newton EC, Goldeski JJ (1982) Factors associated with correct antemortem diagnosis of major pulmonary embolism. *Am J Med* 73:822–826
45. Rubio-Jurado B, Albores-Arguijo RC, Guerra-Soto A, Plasencia-Ortiz T, Tavarez-Macías G, Huerta-Hernández J et al (2020) Concordance between clinical diagnosis of pulmonary thromboembolism at hospital discharge and anatomopathological diagnosis. *Int J Immunopathol Pharmacol* 34:2058738420942390
46. Timmons S, Kingston M, Hussain M, Kelly H, Liston R (2003) Pulmonary embolism: differences in presentation between older and younger patients. *Age Ageing* 32:601–605
47. Berman AR, Arnsten JH (2003) Diagnosis and treatment of pulmonary embolism in the elderly. *Clin Geriatr Med* 19:157–175
48. Paraskos JA, Adelstein SJ, Smith RE, Rickman FD, Grossman W, Dexter L, Dalen JE (1973) Late prognosis of acute pulmonary embolism. *N Engl J Med* 239:55–58
49. Stein PD, Athanasoulis C, Alavi A, Greenspan RH, Hales CA, Saltzman HA, Vreim CE, Terrin ML, Weg JG (1992) Complications and validity of pulmonary angiography in acute pulmonary embolism. *Circulation* 85:462–468
50. Righini M, Le Gal G, De Lucia S, Roy PM, Meyer G, Aujesky D, Bounameaux H, Perrier A (2006) Clinical usefulness of D-dimer testing in cancer patients with suspected pulmonary embolism. *Thromb Haemost* 95:715719
51. Douma RA, Mos IC, Erkens PM, Nizet TA, Durian MF et al (2011) Performance of 4 clinical decision rules in the diagnostic management of acute pulmonary embolism: a prospective cohort study. *Ann Intern Med* 154:709718
52. Miron MJ, Perrier A, Bounameaux H, de Moerloose P, Slosman DO, Didier D, Junod A (1999) Contribution of noninvasive evaluation to the diagnosis of pulmonary embolism in hospitalized patients. *Eur Respir J* 13:13651370
53. Chabloz P, Reber G, Boehlen F, Hohlfeld P, De Moerloose P (2001) TAFI antigen and D-dimer levels during normal pregnancy and at delivery. *Br J Haematol* 115(1):150–152
54. Bajc M, Schümichen C, Grüning T, Lindqvist A, Le Roux PY, Alatri A et al (2019) EANM guideline for ventilation/perfusion single-photon emission computed tomography (SPECT) for diagnosis of pulmonary embolism and beyond. *Eur J Nucl Med Mol Imaging* 46(12):2429–2451
55. Schoepf UJ, Goldhaber SZ, Costello P (2004) Spiral computed tomography for acute pulmonary embolism. *Circulation* 109:2160–2167

56. Radan L, Mor M, Gips S, Schlang-Eisenberg D, Lurie Y, Dickstein K, Bitterman H, Ben-Haim S (2004) The added value of spiral computed tomographic angiography after lung scintigraphy for the diagnosis of pulmonary embolism. *Clin Nucl Med* 29:255–261
57. Wiener RS, Schwartz LM, Woloshin S (2013) When a test is too good: how CT pulmonary angiograms find pulmonary emboli that do not need to be found. *BMJ* 347:3368
58. Aviram G, Levy G, Fishman JE, Blank A, Graif M (2004) Pitfalls in the diagnosis of acute pulmonary embolism on spiral computed tomography. *Curr Probl Diagn Radiol* 33:74–84
59. Perrier A (2001) Pulmonary embolism: from clinical presentation to clinical probability assessment. *Semin Vasc Med* 1:147–154
60. Kanne JP, Lalani TA (2004) Role of computed tomography and magnetic resonance imaging for deep venous thrombosis and pulmonary embolism. *Circulation* 109(12 Suppl 1):115–121
61. Mitchell AM, Kline JA (2007) Contrast nephropathy following computed tomography angiography of the chest for pulmonary embolism in the emergency department. *J Thromb Haemost* 5:50–54
62. Smith-Bindman R, Lipson J, Marcus R et al (2009) Radiation dose associated with common computed tomography examinations and the associated lifetime attributable risk of cancer. *Arch Intern Med* 169:2078–2086
63. Altes TA, Mai VM, Munger TM, Brookeman JR, Hagspiel KD (2005) Pulmonary embolism: comprehensive evaluation with MR ventilation and perfusion scanning with hyperpolarized helium-3, arterial spin tagging, and contrast-enhanced MRA. *J Vasc Interv Radiol* 16:999–1005
64. Mudge CS, Healey TT, Atalay MK, Pezzullo JA (2013) Feasibility of detecting pulmonary embolism using noncontrast MRI. *Radiology* 2013:1–5
65. Benson DG, Schiebler ML, Repplinger MD, François CJ, Grist TM, Reeder SB, Nagle SK (2017) Contrast-enhanced pulmonary MRA for the primary diagnosis of pulmonary embolism: current state of the art and future directions. *Br J Radiol* 90(1074):20160901. <https://doi.org/10.1259/bjr.20160901>. Epub 2017 Apr 12. PMID: 28306332; PMCID: PMC5602179
66. Biello DR, Mattar AG, McKnight RC, Siegel BA (1979) Ventilation-perfusion studies in suspected pulmonary embolism. *AJR Am J Roentgenol* 103:1033–1037
67. Hull RD, Hirsh J, Carter CJ, Jay RM, Dodd PE, Ockelford PA, Coates G, Gill GJ, Turpie AG, Doyle DJ, Buller HR, Raskob GE (1983) Pulmonary angiography, ventilation lung scanning, and venography for clinically suspected pulmonary embolism with abnormal perfusion lung scan. *Ann Intern Med* 98:891–899
68. Onyedika C, Glaser JE, Freeman LM (2010) Pulmonary embolism: role of ventilation-perfusion scintigraphy. *Semin Nucl Med* 43(2):82–87
69. Freeman LM, Glaser JE, Haramati LB (2012) Planar V/Q imaging for pulmonary embolism: the case for “outcomes” medicine. *Semin Nucl Med* 42(1):3–10
70. Burns SK, Haramati LB (2012) Diagnostic imaging and risk stratification of patients with acute pulmonary embolism. *Cardiol Rev* 20:15–24
71. Stein PD, Coleman ER, Gottscalk A, Saltzman H, Terrin ML, Weg JG (1991) Diagnostic utility of ventilation/perfusion lung scans in acute pulmonary embolism is not diminished by pre-existing cardiac or pulmonary disease. *Chest* 100:604–606
72. Harris B, Bailey D, Miles S, Bailey E, Rogers K, Roach P, Thomas P, Hensley M, King GG (2007) Objective analysis of tomographic ventilation–perfusion scintigraphy in pulmonary embolism. *Am J Respir Crit Care Med* 175:1173–1180
73. Bajc M, Neilly JB, Miniati M, Schuemichen C, Meignan M, Jonson B (2009) EANM guidelines for ventilation/perfusion scintigraphy. Part 1. Pulmonary imaging with ventilation/perfusion single photon emission tomography. *Eur J Nucl Med Mol Imaging* 36:1056–1070
74. Glaser JE, Chamarthy M, Haramati LB, Esses D, Freeman LM (2011) Successful and safe implementation of a trinary interpretation and reporting strategy for V/Q lung scintigraphy. *J Nucl Med* 52:1508–1512
75. Sostman HD, Pistolesi M (2011) Scintigraphy for pulmonary embolism: too old to rock ‘n’ roll, too young to die? *J Nucl Med* 52:11A–12A
76. Bhargavan M, Sunshine JH, Lewis RS, Jha S, Owen JB, Vializ J (2010) Frequency of use of imaging tests in the diagnosis of pulmonary embolism: effects of physician specialty, patient characteristics, and region. *AJR Am J Roentgenol* 194:1018–1026
77. The Task Force for the Diagnosis and Management (2008) Guidelines on the diagnosis and management of acute pulmonary embolism. *Eur Heart J* 29:2276–2315
78. Wazir JF, Ansari NA (2004) Pneumocystis carinii infection: update and review. *Arch Pathol Lab Med* 128:1023–1027
79. Feldman C (2005) Pneumonia associated with HIV infection. *Curr Opin Infect Dis* 18:165–170
80. Morris A, Lundgren JD, Masur H, Walzer PD, Hanson DL, Frederick T, Huang L, Beard CB, Kaplan JE (2004) Current epidemiology of Pneumocystis pneumonia. *Emerg Infect Dis* 10:1713–1720
81. Medrano FJ, Montes-Cano M, Conde M, de la Horra C, Respaliza N, Gasch A, Perez-Lozano MJ, Varela JM, Calderon EJ (2005) Pneumocystis jirovecii in general population. *Emerg Infect Dis* 11:245–250
82. Al Soub H, Taha RY, El Deeb Y, Almaslamani M, Al Khuwaiter JY (2004) Pneumocystis carinii pneumonia in a patient without a predisposing illness: case report and review. *Scand J Infect Dis* 36:618–621
83. Kramer EL, Sanger JJ (1989) Detection of thoracic infections by nuclear medicine techniques in the acquired immunodeficiency syndrome. *Radiol Clin N Am* 27:1067–1075

84. Woolfenden JM, Carrasquillo JA, Larson SM, Simmons JT, Masur H, Smith PD, Shelhamer JH, Ognibene FP (1987) Acquired immunodeficiency syndrome: Ga-67 citrate imaging. *Radiology* 162:383–387
85. Raghu G, Collard HR, Egan JJ, Martinez FJ, Behr J et al (2011) An official ATS/ERS/JRS/ALAT statement: idiopathic pulmonary fibrosis: evidence-based guidelines for diagnosis and management. *Am J Respir Crit Care Med* 183:788–824
86. Travis WD, Costabel U, Hansell DM, King TE Jr, Lynch DA et al (2013) An official American Thoracic Society/European Respiratory Society statement: update of the international multidisciplinary classification of the idiopathic interstitial pneumonias. *Am J Respir Crit Care Med* 188:733–748
87. Noble PW, Homer RJ (2004) Idiopathic pulmonary fibrosis: new insights into pathogenesis. *Clin Chest Med* 25:749–758
88. Line BR, Fulmer JD, Reynolds HY, Roberts WC, Jones AE, Harris EK, Crystal RG (1978) Gallium-67 citrate scanning in the staging of idiopathic pulmonary fibrosis: correlation with physiologic and morphologic features and bronchoalveolar lavage. *Am Rev Respir Dis* 118:355–365
89. Baughman RP (2004) Pulmonary sarcoidosis. *Clin Chest Med* 25:521–530
90. Culver DA, Valeyre D (2016) Emerging ideas about sarcoidosis pathophysiology. *Curr Opin Pulm Med* 22:466–468. <https://doi.org/10.1097/MCP.0000000000000310>
91. Mandel J, Weinberger SE (2001) Clinical insights and basic science correlates in sarcoidosis. *Am J Med Sci* 321:99–107
92. ACCESS Research Group (1999) Design of a case control etiologic study of sarcoidosis (ACCESS). *J Clin Epidemiol* 52:1173–1186
93. Scadding JG (1961) Prognosis of intrathoracic sarcoidosis in England. *Br Med J* 4:1165–1172
94. Gupta RG, Beckerman C, Silcian L et al (1982) Gallium citrate scanning and serum angiotensin converting enzyme levels in sarcoidosis. *Radiology* 144:895–899
95. Prabhakar HB, Rabinowitz CB, Gibbons FK, O'Donnell WJ, Shepard JA, Aquino SL (2008) Imaging features of sarcoidosis on MDCT, FDG PET, and PET/CT. *AJR Am J Roentgenol* 190:s1–s6
96. Elgazzar AH, Silberstien EB, Hughes J (1995) Perfusion and ventilation scans in patients with diffuse obstructive airway disease: utility of single breath (wash in) xenon-103. *J Nucl Med* 36:64–67
97. Anthonisen NR, Martin RR (1977) Regional lung function in pleural effusion. *Am Rev Respir Dis* 116:201–207
98. American Cancer Society (2013) Cancer fact & figures. American Cancer Society, Atlanta, p 2013
99. Higashi K, Ueda Y, Sakuma T et al (2001) Comparison of [(18)F]FDG PET and (201)Tl SPECT in evaluation of pulmonary nodules. *J Nucl Med* 42:1489–1496
100. Tümkaya E, Büyükdereli G (2013) The role of F-18-FDG PET and PET/CT in lung cancer. *Arch Med Rev J* 22:470–485
101. Kristersson S (1974) Prediction of lung function after lung surgery. A Xe-133 radiospirometric study of regional lung function in bronchial cancer. *Scand J Thorac Cardiovasc Surg* 18(Suppl):5–44